Faculdade de Engenharia da Universidade do Porto

Biomechanical Simulation of the Damage on the ACL in Injury Related Movements

Marcelo Correia Fonseca

Porto, June 2020

Faculdade de Engenharia da Universidade do Porto

Biomechanical Simulation of the Damage on the ACL in Injury Related Movements

Marcelo Correia Fonseca

Dissertation carried out under the
Masters in Biomedical Engineering

Supervisor: Marco Paulo Lages Parente
Co-Supervisor: João Pedro Sousa Ferreira

Porto, June 2020

Resumo

O ligamento cruzado anterior tem um papel fulcral na estabilização da articulação do joelho. Como consequência, este é um dos ligamentos mais importantes do corpo humano, uma vez que é crucial para a execução dos movimentos precisos e fluídos que os membros inferiores necessitam de executar para a locomoção bípede.

As lesões neste ligamento têm consequências catastróficas e podem resultar em deficiências graves e causar ainda mais lesões devido à instabilidade que geram na articulação. Os atletas são especialmente vulneráveis devido ao elevado nível de atividade física nas suas vidas. As lesões neste ligamento exigem longos períodos de recuperação e, em alguns casos, podem resultar num fim prematuro da carreira desportiva. O ligamento cruzado anterior é das estruturas do corpo humano com maior propensão a lesões, sendo que a maioria destas lesões ocorre sem a necessidade de contacto físico, estas acontecem devido a um movimento que a pessoa efetua e que impõe tensões extremas no ligamento.

Para prevenir este tipo de lesão é primeiro necessário compreender exatamente como acontecem, apenas assim podem ser identificados e evitados os fatores de risco. Estas lesões ocorrem normalmente em atletas que participam em desportos que envolvem movimentos de saltos, rotações, trocas de direção e acelerações e desacelerações súbitas. Contudo, até agora, o mecanismo por trás da lesão deste ligamento ainda não é totalmente compreendido.

Devido às dificuldades associadas à medição direta de deformações no LCA quando uma pessoa está em movimento, a análise por elementos finitos tem sido usada para simular estes movimentos em modelos computacionais e estudar o ligamento e lesões associadas. Assim sendo, este trabalho tem como objetivo o estudo da rutura do ligamento cruzado anterior. Para tal, um modelo de elementos finitos estável foi desenvolvido de modo a incluir uma “user material subroutine” que atribuiu o modelo material de Holzapfel-Gasser-Ogden ao LCA, assim como, um parâmetro de dano, criado para tecidos moles biológicos e fibrosos, permitindo estimar a localização e extensão do dano nas fibras de colagénio. Com isto, vários movimentos associados à lesão do LCA foram testados e os resultados obtidos foram satisfatórios, uma vez que, encontram-se de acordo com o expectável.

Abstract

The anterior cruciate ligament (ACL) performs a vital role in the stabilization of the knee joint. This makes it one of the most important ligaments in the human body, since it is crucial for the execution of the precise and fluid motions that the lower limbs are required to perform for bipedal locomotion.

Injuries to this ligament have catastrophic consequences and can result in serious disability and further injuries caused by the instability that is derived from it. Athletes are especially vulnerable due to the high level of physical activity in their lives. Injuries to the ACL can require large periods of recovery time and, in some cases, may result in a premature end of an athletic career. The ACL is one of the most commonly injured structures in the human body. Most of these injuries require no physical contact, they occur due to a movement that a person performs which imposes extreme strains on this ligament.

In order to prevent this type of injury it is necessary to first understand exactly how it happens, only then can the risk factors be identified and prevented. It is known to usually occur in athletes who participate in sports that involve pivoting, cutting, jumping movements or sudden accelerations and decelerations. However, to this day, the mechanism behind the ACL injury remains to be fully understood.

Due to the difficulties of directly measuring the strains on the ACL when a person is moving, finite element analysis have been employed to simulate these movements on computational models and study the ligament and the injuries associated with it. As such, this work sets out to study the ACL rupture. For this purpose, a stable finite element model was developed which included a user material subroutine that attributed the Holzapfel-Gasser-Ogden material model to the ACL and also had the inclusion of a damage parameter, designed for fibrous biological soft tissues, which allowed to estimate the location and extent of the damage to the collagen fibres. With it, several movements associated with the ACL injury were tested and the obtained results were satisfying since they were in accordance with what was expected.

Agradecimentos

Em primeiro lugar tenho de agradecer ao meu orientador, Professor Doutor Marco Parente, pela oportunidade, mas acima de tudo pela paciência, disponibilidade e apoio que demonstrou desde o primeiro dia. Por arranjar sempre maneira de tirar uma dúvida ou ajudar na resolução de um problema, mesmo quando tinha um horário ocupado. Pelos inúmeros emails e várias reuniões, que mais tarde se transformaram em videochamadas, todas elas indispensáveis para a realização deste projeto. Por todo este apoio, dado sempre com enorme simpatia e sem nunca faltar uma palavra de incentivo, um muito obrigado.

Tenho também de agradecer ao João Ferreira pela ajuda que prestou nestes últimos meses, que acabou por ser também essencial para este trabalho. Por ter estado presente e disposto a ajudar sempre que era necessário e por nunca deixar de me encorajar e de oferecer a sua valiosa opinião para a resolução de diversos problemas que foram surgindo com os resultados obtidos.

À minha namorada Inês por ser também a minha melhor amiga e por ser a pessoa com quem posso sempre contar para me apoiar, tanto a nível académico como a nível pessoal. Por tudo o que fazes por mim e por seres como és, muito obrigado.

Aos meus pais e ao meu irmão por me terem acompanhado e incentivado nesta viagem académica e que, mesmo à distância, nunca deixaram de estar presentes ou de me ajudar.

Por fim, tenho ainda de deixar uma palavra de agradecimento ao Guilherme e ao Pedro, à Rita, Sara e Sandra pelos momentos inesquecíveis e pela forte amizade ao longo de todos estes anos.

Contents

List of Figures

List of Tables

List of Abbreviations and Symbols

Abbreviations

3D	Three-Dimensional
ACL	Anterior Cruciate Ligament
AM	Anteromedial
FEM	Finite Element Method
HGO	Holzapfel-Gasser-Ogden
LCL	Lateral Collateral Ligament
MCL	Medial Collateral Ligament
Pa	Pascal
PCL	Posterior Collateral Ligament
PL	Posterolateral
UMAT	User Material

Symbols

$\mathbf{B}$	Left – Cauchy Green tensor
$\mathbf{C}$	Right – Cauchy Green tensor
$\mathbf{F}$	Deformation gradient
$\mathbf{T}$	Nominal Piola – Kirchhoff traction vector
$\mathbf{P}$	First Piola – Kirchhoff stress tensor
$\mathbf{S}$	Piola Kirchhoff tensor
$\mathbf{\Sigma}$	Second Piola Kirchhoff stress tensor
$\boldsymbol{\sigma}$	Stress
$\boldsymbol{\varepsilon}$	Strain
$\mathbf{u}$	Displacement
$\mathbf{e}$	Eulerian stress tensor
$\mathbf{t}$	Traction vector
$\boldsymbol{\tau}$	Kirchhoff stress

Chapter 1 - Introduction

1.1 - Framework

The knee is one of the largest and most complex joints of the human body. It is essential for providing the necessary mobility for bipedal locomotion, being capable of supporting the loads imposed by the weight of the body while carrying out precise and fluid movements with great stability [1]. This can only be achieved due to the complex geometry of the knee joint and its several anatomical structures which include cartilages, menisci and ligaments. However, this delicate system can be compromised by injuries, which alter the load distribution along the joint which causes pain and can result in additional injuries to other structures or even in long term disability [2, 3].

Injuries to the ligaments of the knee are quite common, especially in active people who engage in sports activities. One of the most important ligaments in the knee is the anterior cruciate ligament (ACL), which plays a crucial role in the stabilization of the joint. However, it is also one of the most commonly injured ligaments in the human body and its injury can have devastating consequences [4]. ACL injuries are expensive to treat because the ligament has a limited ability for self-repair and when it suffers an injury, it is often incapable of recovering on its own and restoring normal knee kinematics, which is why these injuries usually require reconstructive surgery or, in case of a full tear, complete surgical replacement [5].

In the United States alone, there are around 150 000 ACL injuries each year, which represent an economic impact of over 500 million dollars [6]. In Norway, the annual incidence of ACL reconstructions from 2004 to 2006 was 85 for every 100 000 citizens between 16 to 39 years old, while in the United Kingdom, ACL injuries have been reported to affect 8.1 in every 100 000 citizens from ages 13 to 89 years old. In fact, it is estimated that 1 million ACL injuries occur every year around the world [7].

Besides the damage to the ligament itself, the instability created by the ACL injury often leads to the appearance of injuries in other knee structures, mainly the menisci and the articular cartilages, as well as, increasing the susceptibility to osteoarthritis [8].

1.2 - Motivation

Over 70% of all ACL injuries occur without any physical contact between the athletes [6]. This means that the most common source of injury is the movements that the athletes perform in their physical activities. Therefore, if it is possible to fully determine the mechanism behind this injury then it would be possible to assess the risk factors that cause it. With this knowledge, it would then be possible to develop workout programs that could help the athletes minimize the probability of sustaining an ACL injury [8].

The ACL injury occurs when an excessive tension is applied to the ligament. Recent research suggests that it is an injury which appears to be caused by a complex interaction of forces and moments [9]. So, in order to fully comprehend the cause of this injury, it is essential to completely understand the mechanism behind the loading of the ACL when a person is active during physical activity [8]. However, measuring the loads that are applied to the ACL when an athlete is in motion is an extremely difficult task since direct access to the ligament is impossible without invasive procedures.

The use of computational mechanics allows for the study of the stresses and displacements within the human body without requiring human subjects and with high accuracy [6]. This is the reason why numerical analyses, namely using the Finite Element Method (FEM), have been widely used in the study of the knee and ACL biomechanics. With these analyses, the mechanism of the noncontact ACL injury has become clearer over time, however, further research is still needed to understand the relevance of the several components that are involved in this condition.

1.3 - Objectives

The objective of this work is to propose a working and accurate finite element model of the ACL, capable of estimating the damage it experiences in injury related movements. For this purpose, a damage parameter will be introduced, using a user material subroutine (UMAT). This model will be subjected to several movements and rotations in order to simulate the joint environment in the movements where ACL injury is most common. The movements that will be tested are the anterior translation of the tibia, knee valgus, knee flexion and tibial internal rotation. Afterwards, several combinations of these movements will be tested. In these simulations, the numerical damage to the fibres and extracellular matrix will be evaluated regarding its onset and extent.

The results are expected to reproduce the behaviour of the ACL in these situations and the damage it sustains. The damage resulting from these movements will be assessed, in regards to its onset and location.

Besides this, the results are expected to support the idea that the ACL injury is the result of a combination of movements, and that some movements generate tensions of higher magnitude on

the ligament, resulting in complete rupture of the fibres and extracellular matrix, while others have a smaller contribution to the overall load.

1.4 – State of the art

The FEM has been used in biomechanics for quite some time and since the knee is one of the most important joints of the human body, it is only natural that such a widely used method would be applied to its study. In fact, the earliest 3D geometric model of the knee using the FEM was created in 1980 (Wismans, *et al.* [10]). The predictions the model offered were in accordance with the experimental data available from the literature, which proved that the application of the FEM to the study of knee biomechanics was a promising approach. Since then, several studies have been performed using this method and several other 3D models of the knee have been developed.

Recently, the FEM has been applied to the study of knee prosthesis [11-13], the functions of some of the anatomical structures that are part of the knee (such as the menisci [14] or the MCL [15]) or even the injuries that afflict this joint, whether by developing models that may help to understand the mechanisms behind these injuries [3], or how an injury to one structure of the knee impacts the remaining structures and the normal functioning of the joint [16].

Since one of the most common and serious conditions that affect the knee are injuries to the ACL, this is a ligament which has been the subject of many studies throughout the years. Finite element models have been used to study the effect of injuries to this ligament on the joint mechanics of the knee [2, 17, 18], to evaluate the effectiveness of new possible treatments to this injury, as in the case of Wang H., *et al.* [19] where the stresses and strains on the ACL were studied in a finite element model which included a ring device which was recently developed to assist in the healing of this ligament. It has also been used to assist in the medical procedures that are employed after an ACL tear, Westermann R.W., *et al.* [20] studied the influence of the size of the graft, used in ACL reconstruction surgeries, on the knee biomechanics and found that grafts of bigger dimensions lead to better biomechanical properties in the recovering knee. While Halonen K.S., *et al.* [21], provided some insight on the optimal graft stiffness and pre-strain that should be considered in these surgeries. Much like the aim of this work, finite element models have also been used in the study of the mechanism injury on this ligament [3, 22, 23].

However, due to the complexity of the knee joint, many of the studies using the FEM use simplified models which focus only on the ligament itself [24, 25] or on the tibiofemoral joint with only the femur, tibia and the ACL [22, 26, 27]. Even in studies where the laborious task of modelling all of the main structures of the knee is undertaken and the models that are used are anatomically complex and similar to the real joint, there are still some challenges which stand in the way of finite element analysis of the ACL:

- The nonlinear anisotropic behaviour of the ligaments is something which cannot yet be completely characterized by any material model [28]. This makes the ligaments of the knee, one of the most difficult structures to simulate, even though they are, due to their vital function in this joint, one of the most important. It is impossible to obtain experimental data

with the level of detail required to calculate the several property values that would be required to precisely recreate ligaments in a simulation [29].

- Achieving a trustworthy validation of a model created using the FEM is a necessary step which is still difficult to achieve. A model is considered to be validated when evidence is provided that the results it generated match the outcomes of a real-world scenario, even if the material properties it uses are not explicitly validated. However, sometimes the outcomes of these real-world scenarios stem from experimental data which has its limitations, especially in the case of *in vivo* subjects, where direct measurement of contact forces in the joint is impossible [29, 30]. This results in a simulation which is created based on the existing literature, but not directly validated.
- Several experimental studies show that the ACL is never in a stress-free state at any degree of knee flexion. However, many finite element models do not take this into account and assume that a stress-free state exists at full knee extension or close to it and as such, fail to accurately replicate the tissue mechanics [25].

Besides this, it should be mentioned that the material properties that are attributed to a finite element analyses are rather important in order to ensure that the results obtained from it, are trustworthy and can be validated. However, since ligaments have material properties that vary from person to person, both Beidokhti H.N., *et al.* [31] and Mootanah, R., *et al.* [32] have found that including subject-specific ligament properties improved the capacity of predicting experimental kinematics and contact pressures. Nonetheless, if the conclusions derived from a model are within an extent that could be sensibly determined using a more generic approach, it is fair to state that a model is validated based on literature comparisons [29].

The FEM has also been used numerous times to characterize soft tissue damage. These damage models date back to the 1970s, however, they still have many limitations since they are based on in vitro measurements and due to the heterogenous and anisotropic behaviour typically associated with these types of materials. Despite their limitations, they are a helpful tool in the understanding of the way these soft tissues are damaged in cases of injuries and even in the fabrication and design of artificial soft tissues [33]. Most of these models have been applied to the study of arteries [34-36], nevertheless, some damage models have been used in the study of ligaments, for example, in the work of Forestiero A. *et al.*, 2014 [37] where the damage of ankle ligaments was studied in the case of an injury. In earlier works there are examples of these models being applied to the knee joint, for example, in the works of De Vita R. *et al.*, 2007 [38] and Guo Z. *et al.*, 2009 [39], where damage models were applied to the study of the medial collateral ligament of the knee.

Chapter 2 - Anatomical Planes and Directions

The focus of this work is on a specific joint of the human body, the knee, and more specifically, one of its ligaments. However, before diving into any details on the knee and any of its structures, it is important to understand the different anatomical directions that come into play when describing the anatomy of the human body.

When talking about the human body, its “conventional anatomical position”, from which all anatomical descriptions stem from, is the standing position while facing forward with the arms by the side and palms facing forward as well [40].

From this position, anatomical descriptions are made based on three different planes, which are shown in Figure 2.1. Sagittal planes, which are vertical and divide the body into a left and a right side, the sagittal plane that is exactly in the midline of the body is called the median plane. The frontal or coronal planes, which divide the body in anterior (front) and posterior (back) sections. Lastly, the transverse or horizontal planes which divide the body in superior and inferior sections [40, 41].

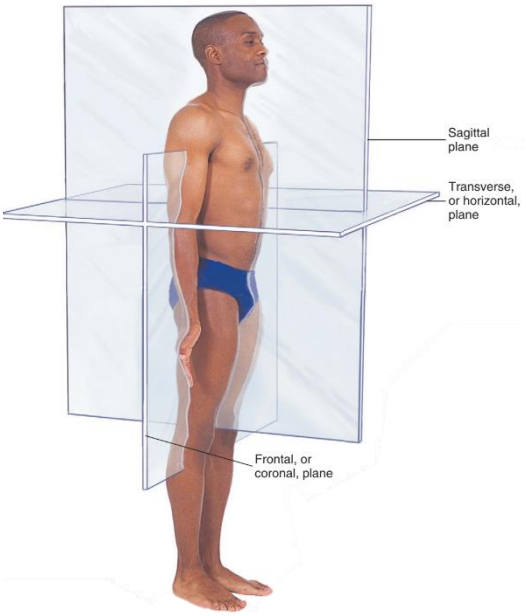

Figure 2.1 – Anatomical planes of the human body [42].

Besides the different anatomical planes that divide the body it is important to understand the directional references that are commonly used. As was previously stated, anterior and posterior refer to the front and back respectively. When considering the midline of the body, lateral refers to the position further away from midline whereas medial refers to the position closest to the midline. Finally, proximal and distal are used to describe structures in the limbs, referring to the point which is closest and furthest, respectively, to the attachment of the limb to the torso [42].

Chapter 3 - Joints

The site where two bones meet is called a joint. These are the weakest parts of the skeleton, nevertheless, they are also responsible for the mobility and stability of the human body. Structurally, there are three different types of joints: fibrous, cartilaginous and synovial [42].

In fibrous joints, the bones are united by fibrous connective tissue, there is no joint cavity, and most of these joints perform little to no movement. An example of this type of joints is the joints in the skull, which are a particular type of fibrous joint called sutures, so called due to their structure [40, 42]. The figure below shows the three different suture joints in the skull, the coronal, sagittal and lambdoid suture.

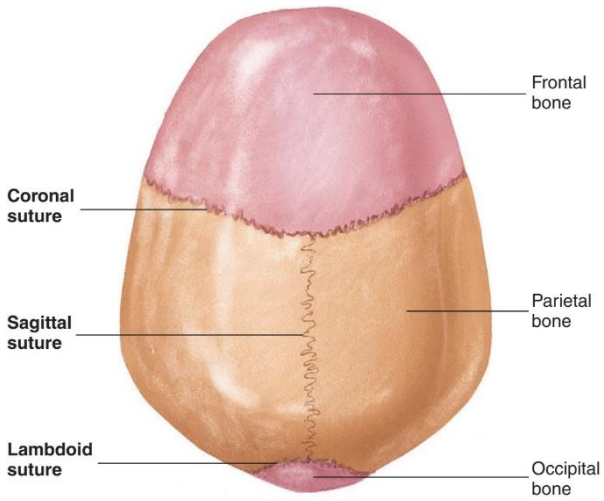

Figure 3.1 – Superior view of the skull which shows the three fibrous joints (sutures) which link its bones [41].

Cartilaginous joints can either have hyaline cartilage (which are called synchondroses) or fibrocartilage (symphyses) between the bones they unite. As in the fibrous joints, this type of joint lacks a joint cavity and the movements it allows for are somewhat limited. An example of cartilaginous joints are the joints in the intervertebral discs, which are made up of fibrocartilage which, due to its strength and compressibility, is ideal as a shock absorber [41, 42].

The third type of joints, the synovial joints, are much more mobile than the other types and are the most common type, especially in the limbs. In these joints, the bones that are articulated, are separated by a joint cavity which is filled with synovial fluid [41]. The articulating surfaces of the bones linked by the joint are covered with a layer of hyaline cartilage (articular cartilage) which smoothens the contact point between the bones and absorbs compression forces. Besides the articular cartilages, these joints are also reinforced with ligaments which are especially important to strengthen them. Some synovial joints may also possess discs of fibrocartilage separating the articular cartilages called articular disks. In some cases, these articular disks are incomplete and form crescent-shaped wedges with a hole in the centre and are called menisci [42, 43]. The general structure of a synovial joint is illustrated in the figure below, where it is possible to see the different components that are present in this type of joint.

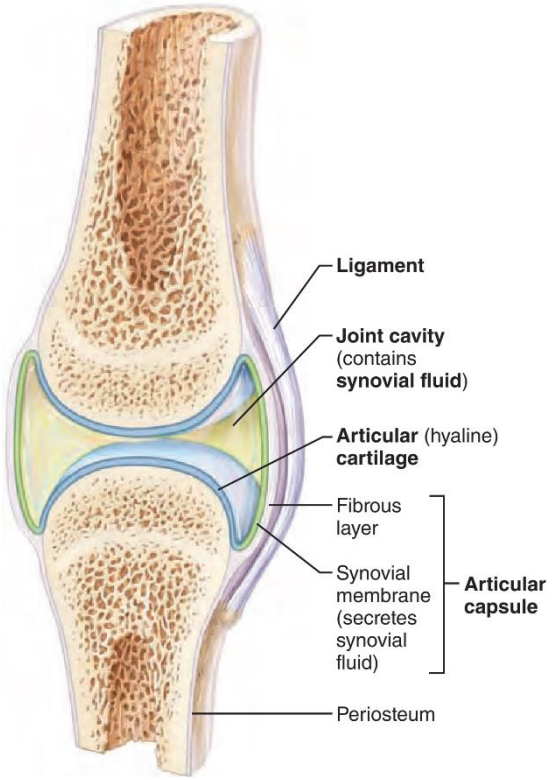

Figure 3.2 – General structure of a synovial joint.

3.1 - Knee Joint

The knee is one of the most important joints of the human body since it is responsible for mobilizing and stabilizing the lower limbs of the human body. It is the largest synovial joint and one which exhibits a high degree of complexity that gives it the capacity to endure impressive loads and perform the precise movements that are required for bipedal locomotion [1].

Even though the knee is made up of a single joint cavity it is, in fact, a combination of three different joints: an intermediate one between the patella and the femur, called the femoropatellar joint, and the lateral and medial joints, which are usually grouped together and given the designation of tibiofemoral joint. These last two joints stand at the two points of contact between each of the femoral condyles and the menisci that are located at the top of the tibia [1].

The tibiofemoral joint, with its lateral and medial components, is responsible for the flexion and extension of the knee. When this flexion occurs, the femoropatellar joint allows for the patella to slide along the distal end of the femur [43]. In an intact knee (Figure 3.3 a) these joints are covered by the patella and the quadriceps tendon. With the removal of the patella from the femoropatellar joint (Figure 3.3 b) the visualization of the inner structures of the knee becomes possible and the tibiofemoral joint is then visible.

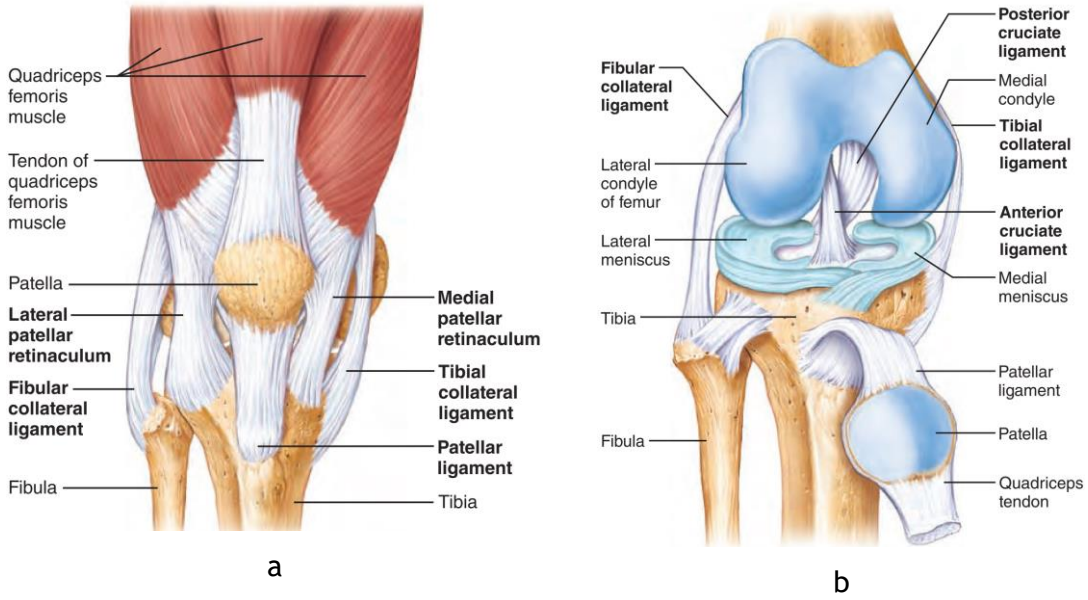

Figure 3.3 – The knee joint: a) Anterior view of the knee; b) Anterior view of flexed knee with cut quadriceps tendon and removal of the patella from its joint [43].

3.1.1 - Anatomy

The main anatomical structures responsible for providing the joint stability and functionality that the knee requires are bones, menisci, ligaments and cartilages. In the following section, these anatomical structures will be presented and their anatomy will be briefly discussed, since having a basic notion of these concepts is crucial in order to fully understand the behaviour of this joint in the movements it performs.

3.1.1.1 - Bones

As was previously mentioned, the knee joint establishes the articulation of the femur with the tibia and the patella. The femur is the longest bone of the human body, in its proximal region it presents a rounded head, while at the distal extremity, where it engages with the knee joint, it forms two condyles, which are separated by the intercondylar notch, and that interact with the tibia in the tibiofemoral joint [1]. In Figure 3.4 it is possible to see the two femoral condyles and their connection with the two correspondent condyles of the tibia, which is in turn the second longest bone of the human body.

The tibia is parallel and articulates with a bone called fibula forming the tibiofibular joint. Even though this joint is represented in Figure 3.4, it does not allow for any movement, neither is it considered to be part of the knee joint. It merely has a support function and acts to stabilize and strengthen the leg [43].

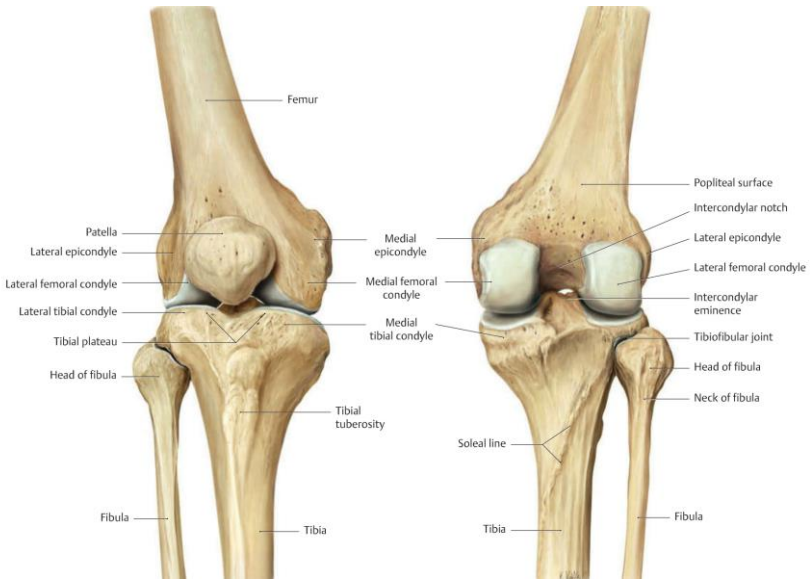

Figure 3.4 – Anterior (left) and posterior (right) view of the bones of the knee joint [44].

Besides the femur and the tibia, the patella constitutes the third bone involved in the knee joint. It is much smaller than the other two and it is a flat bone which is embedded in the tendon of the quadriceps muscle [41]. Despite its small size, it has two rather important functions: it acts as a protective surface to the knee joint and plays a vital role in the extensor mechanism of the knee, as it is responsible for increasing the extensile strength by up to 50% [45].

3.1.1.2 - Menisci

The menisci are two fibrocartilaginous structures that are located on tibiofemoral joint and that increase the articular surface of the tibia in the articulation with the femoral condyles. The medial meniscus is shaped like a C letter and while it is broader than the lateral meniscus, it is a bit thinner. The lateral meniscus has a more circular shape and does not open as widely to the intercondylar eminence as the medial meniscus [45]. The anatomy of both menisci is represented in Figure 3.5.

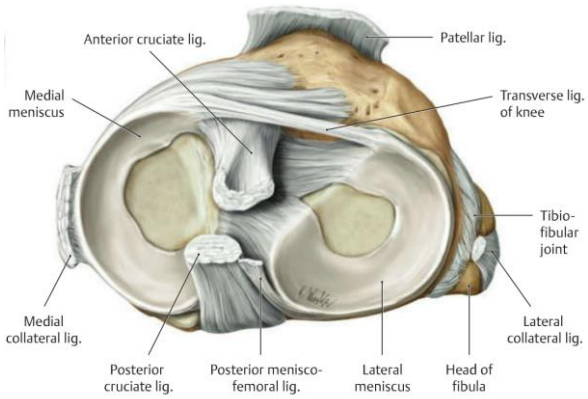

Figure 3.5 – Menisci in the knee joint [44].

Owing to their complex anatomy, the menisci are capable of performing several functions, the most evident one is the cushioning from the loads that are exerted on the knee joint and being responsible for increasing the contact area between the femur and the tibia [46]. This is visible in Figure 3.6, where in the absence of these structures the compressive loads are less distributed increasing the stress on the articular cartilage, which explains the prevalence of osteoarthritis following meniscectomy [1]. Besides this, the menisci also play a role in guiding rotation and stabilizing translation movements [46].

These are dynamic structures capable moving along with the femur and the tibia in order to keep up with the movements that the knee joint performs, without compromising its balance. This way, the menisci are capable of optimizing their function as load bearing units [47, 48].

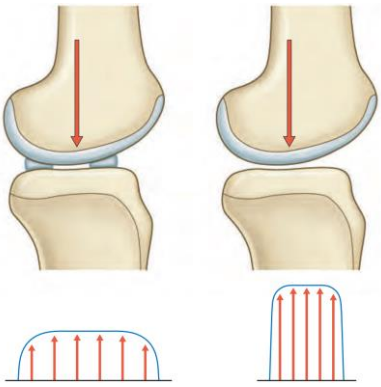

Figure 3.6 – Influence of the menisci in increasing the contact area and distributing the compressive forces.

3.1.1.3 - Ligaments

Ligaments are bands of fibrous connective tissue which establish connections between bones and reinforce joints, facilitating the movements that are required for the normal motion of the human body, while at the same time, restricting undesirable motions in other directions [43].

Despite the presence of several ligaments in the knee, the most important ones are the two cruciate ligaments (anterior and posterior), named this way because they cross each other, and the medial and lateral collateral ligaments [4]. These structures are represented in the figure below, where the two cruciate ligaments are seen between the femur and the tibia, and where, on both sides of the knee joint, the two collateral ligaments are visible.

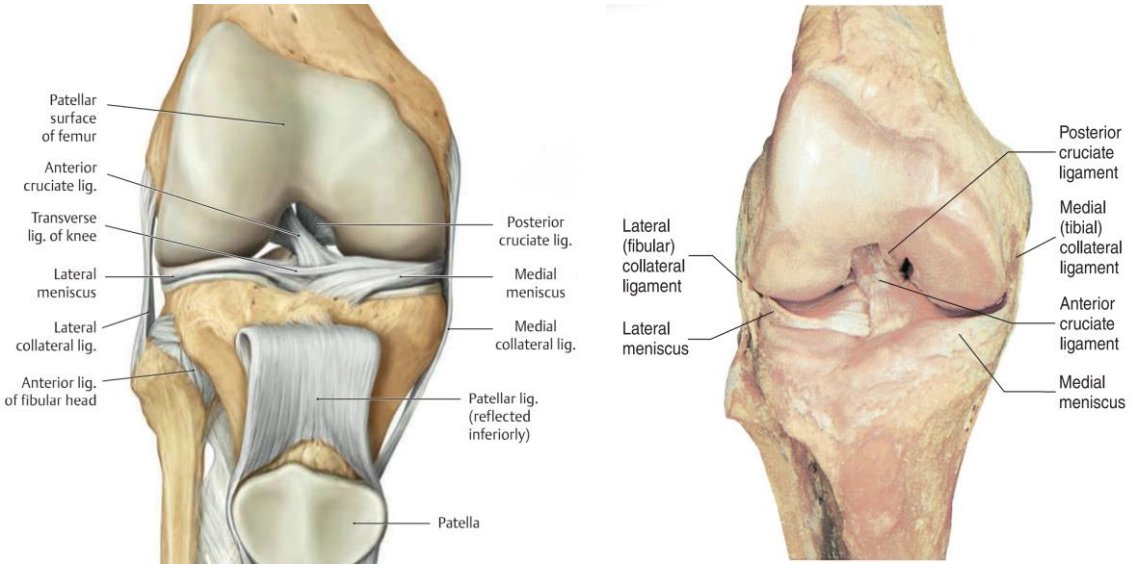

a) b)

Figure 3.7 - a) Anterior view of the knee joint and its ligaments [44]; b) Photograph of anterior view of the knee [41].

Ligaments are made up of tightly packed bundles of oriented collagen fibres whose function is to provide support to the multiple joints that make up the musculoskeletal system. The main component of the ligaments is type I collagen, which is around 70-80% of their dry weight, the rest is almost exclusively type III and V collagen although, other collagen types have also been found to be incorporated in these structures [4].

The ACL is a ligament of paramount importance in stabilizing the knee joint since it prevents anterior tibial translation in relation to the femur and has a significant role in resisting rotational loads. Due to its limited capacity of repairing itself and the fact that it is rather frequently torn during sport related movements, it was chosen to be the focus of this work. Its anatomy and biomechanics will be further discussed in Chapter 4 [5, 49].

As was previously mentioned there are two cruciate ligaments, one is the ACL and the other is the posterior cruciate ligament (PCL). The PCL is in turn responsible for preventing posterior translation of the tibia in relation to the femur while also acting to stabilize the knee in rotational loads [50]. Its origin is in the medial surface of the intercondylar notch of the femur and projects itself to a depression in the intercondylar eminence of the tibia. It is made up of two bundles, the larger anterolateral bundle, which is tight in flexion, and the smaller posteromedial unit, which in turn is tight in extension. As a whole, the PCL has a greater cross-sectional area than the ACL and is therefore stronger [45]. Another distinction from the ACL is the fact that unlike its counterpart, the blood supply to the PCL is not permanently lost in case of substantial tear, which gives it an enhanced ability of self-repair, making injuries that affect this ligament less problematic [46].

Besides the cruciate ligaments, there are two main ligaments that act as stabilizers to the joint: the medial collateral ligament (MCL) and the lateral collateral ligament (LCL), which are tight when the knee is in extension and act to stabilize the medial and lateral sides of the knee, respectively. The MCL has its origin in the lateral femoral epicondyle and attaches to the head of the fibula, while the LCL originates in the medial epicondyle of the femur and attaches to medial surface of the tibia [41]. Both are crucial to limit the internal and external rotations of the knee [46]. The figure below is a representation of both sides of the knee where the two collateral ligaments are visible.

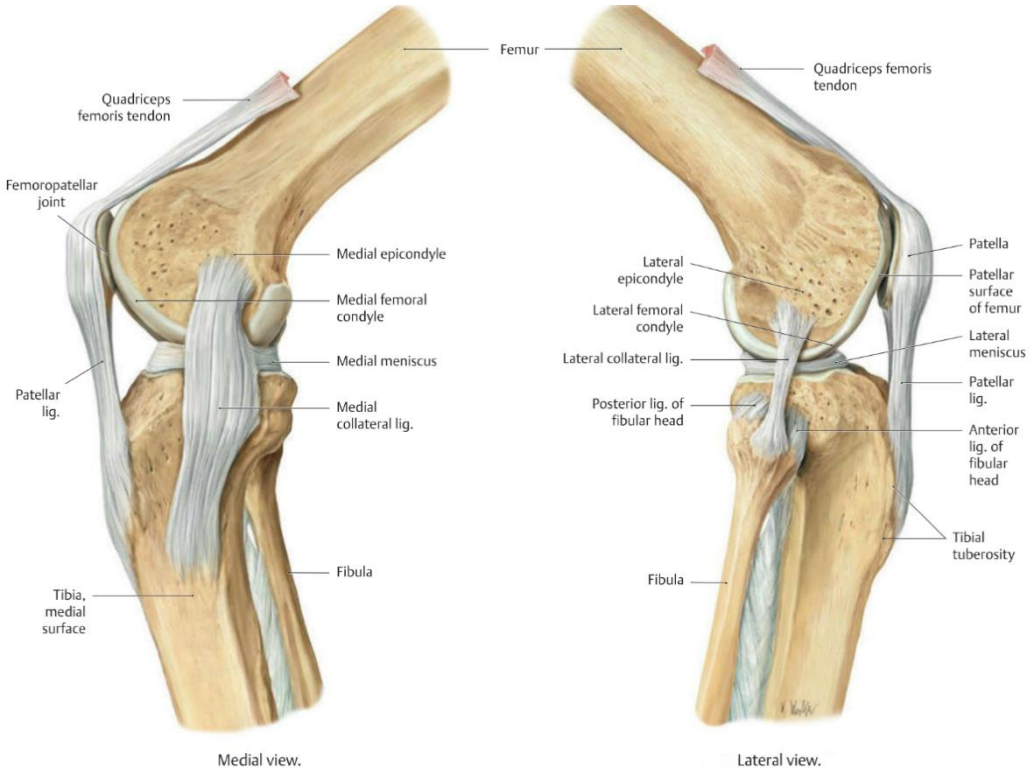

Figure 3.8 – Medial and lateral views of the knee with emphasis on the collateral ligaments [44].

3.1.1.4 - Articular Cartilages

Besides the fibrocartilaginous menisci, there are articular cartilages that cover the femoral and the tibial condyles, providing a surface with minimal attrition, which allows for joint movement. They also perform an important part when it comes to load absorption, which is crucial for preventing the bones from damaging each other due to the powerful loads that the knee is subjected to, from the body and the dynamic movements it performs [51].

There are three articular cartilages in the knee joint, one covering the femoral extremity, another on the tibial extremity and one on the patella [51], as can be seen in the figure below, where the cartilages are represented in white.

Figure 3.9 - Articular cartilages of the knee [52].

3.1.2 - Biomechanics

Biomechanics is defined as the science that studies the forces and movements in biological systems [53]. In order to successfully study the interactions of the several components of the knee joint, during the movements it performs, one must first comprehend them.

When oversimplifying the matter, the knee may be described as a complex hinge joint which allows for flexion and extension, along with some rotational motions. In fact it has six degrees of motion, which may be classified as three rotations (flexion-extension, external-internal rotation, varus-valgus angulation) and three translations (anterior-posterior glide, medial-lateral shift, compression-distraction) [54, 55], as can be seen in the figure below.

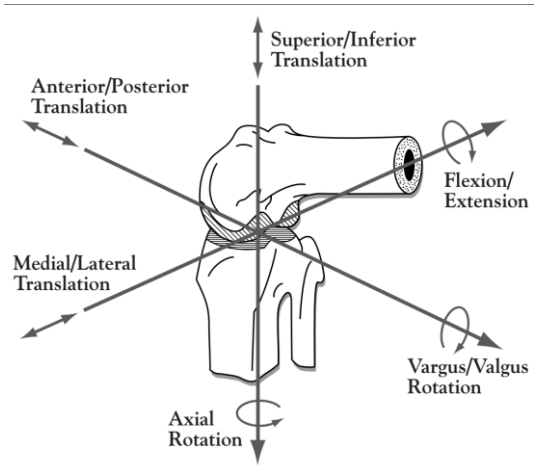

Figure 3.10 - The six degrees of motion of the knee [54].

Another way of visualizing the knee motion with its six degrees of freedom, is to relate the movement, in this case the translations and rotations, to three axis in the knee: the tibial axis (proximal-distal translation and internal-external rotation), the epicondylar axis (medial-lateral

translation and flexion extension) and the anteroposterior axis (antero-posterior translation and varus-valgus rotation) (Figure 3.11) [53].

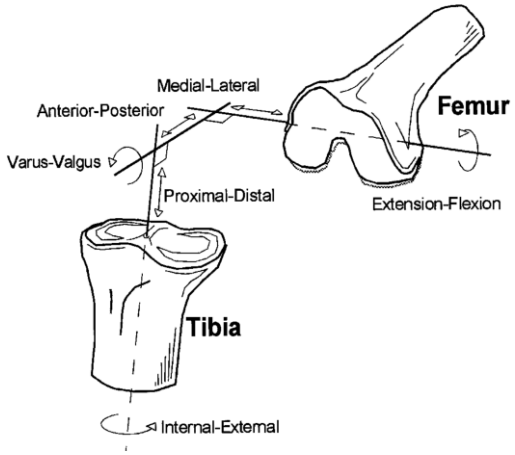

Figure 3.11 – Six degrees of motion of the knee in relation to the tibial, epicondylar and anteroposterior axis [53].

The movements of the knee are often considered to start at 0°, which is defined as the neutral position, the position where the tibia is aligned with the femur. This is the position of full extension, which defines one of the most important functions of the knee, the ability to support the body while standing still. Here, the knee is fixed, and the thigh and leg muscles can relax without compromising stability. If this alignment of the tibia and femur in the sagittal plane was not possible, and the knee was slightly flexed when standing still, the body would tend to tilt posteriorly, which would only be prevented by contracting the quadriceps muscle at the continuous expense of energy [1].

The main movement of the knee joint is extension/flexion and involves the tibiofemoral joint. It usually occurs between 0° and 130°, although in some cases it may surpass 130°, depending on the mass of the posterior thigh and calf muscles which limit this movement [1]. During the flexion movement there is also a combination of movements occurring between the femoral condyles and the tibia, including sliding, rolling and rotation. Knee flexion is initiated by the popliteus muscle which rotates the femur in respect to the tibia and disrupts the position of full extension. In the beginning of the flexion (near complete extension, 0°-20°) rolling of the tibiofemoral joint is predominant, while after a flexion angle of 30°, sliding becomes dominant (Figure 3.12) [1, 56].

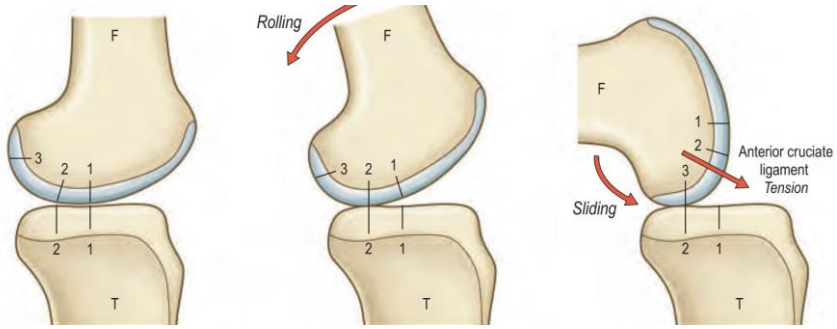

Figure 3.12 – Sliding and rolling motions in the flexion movement of the knee joint. Left- Full extension, the centre of the femur (F1) aligns with the centre of the tibia (T1). Middle – Rolling at the beginning of the flexion (contact shifts from F1-T1 to F2-T2). Right- Deep flexion, the ACL prevents further rolling so the femur slides on the tibia (F3 moves to T2) [1].

Due to an asymmetry between the medial and lateral femoral condyles, the rolling motion on the lateral condyle is more accentuated than in the medial condyle which leads to external rotation of the tibia during the extension movement. This rotation leads to a tightening of the ACL and eventually "locks" the knee in the fully extended position. Gliding predominantly occurs in the medial condyle and, therefore, during the flexion of the knee the tibia internally rotates [57, 58].

As was mentioned before, the cruciate ligaments play a vital part in the stabilization of the knee. During knee flexion the ACL becomes more relaxed, and the PCL tightens, while in knee extension the opposite occurs. These slackening and tensioning sequences are associated with changes in ligament orientation with the ACL changing from a vertical to a more horizontal orientation with knee flexion, while the opposite occurs with the PCL [45]. Since the ligaments compensate for tensile stresses that act in line with the axis of their collagen fibres, this change in orientation provides the required dynamic stability to the sagittal plane of the knee. In fact, damage to these ligaments was found to be accompanied by increased physiological stress to other joints in the body due to the resulting imbalances in the sagittal axis of rotation [57].

Medial and lateral stability of the knee joint is mainly attributed to the collateral ligaments, without which the cruciate ligaments would be unable to withstand the varus/valgus stresses during the motions of the joint [45]. The MCL is the primary restraint to valgus rotation, while also aiding in limiting external rotation and straight medial and lateral translation of the tibia. The LCL is the primary restraint to varus rotations and acts as a secondary restraint to external rotation and posterior translation [50].

Chapter 4 - Anterior Cruciate Ligament

As was previously mentioned, the ACL is an anatomical structure of the utmost importance in the knee joint. Its anatomy and biomechanical significance has already been discussed in 3.1.1.3, along with that of several other anatomical structures of this joint. However, since the aim of this work is to study sport related injuries that affect this specific ligament, in this section, its anatomy and biomechanics will be further explored in greater detail.

4.1 - Anatomy

The ACL originates on the posterior medial area of the lateral femoral condyle, it then runs anteriorly, medially and distally from the femur to the tibia, while spiralling laterally on itself. The tibial attachment is wider and stronger than the femoral one [5].

The ACL function cannot be reduced to a simple tube of fibres at constant tension, it rather consists of groups of fibres that are subjected to lengthening and slackening episodes. With this in mind, there is often a need to divide the ACL into two functional subdivisions: the anteromedial (AM) and the posterolateral (PL) bundles (Figure 4.1) [57]. These two bundles wrap around each other, with the AM bundle being longer than the PL. Functionally, these two bundles act differently with the movement of the knee. At knee extension, both are parallel and relatively tense, nevertheless, as the knee increases its flexion, the AM bundle stays relatively taut while the PL bundle becomes relaxed [5]. Either way, the ACL is a ligament that is always under some tension, at least in one of its portions [25].

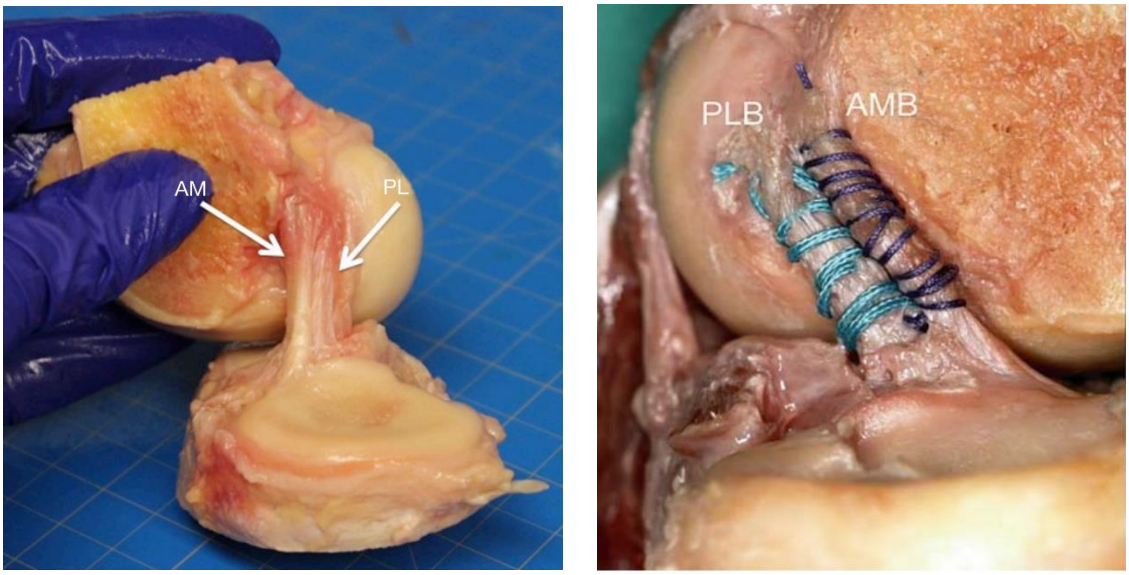

Figure 4.1 – AM and PL bundles of the ACL (left) [59]; ACL with its two bundles identified with different colours (right) [60].

At full extension, which is how femoral origins are normally described through an anatomical point of view, the femoral attachment of the AM bundle is at the proximal portion of the ACL, while the attachment of the PL bundle stands posterior and distal to it (Figure 4.2 A). However, at knee flexion, the PL attachment becomes more anterior to the AM attachment (Figure 4.2 B) [61].

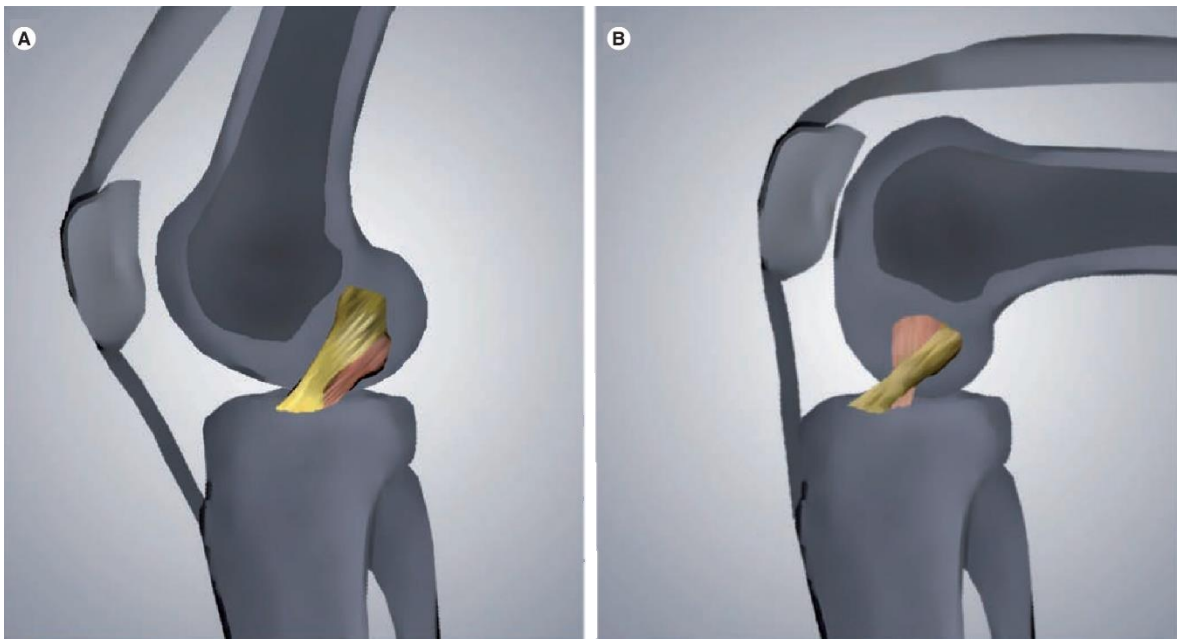

Figure 4.2 – AM bundle (light grey) and PL bundle (dark grey) at knee extension (A) and knee flexion (B) [61].

Other bundles besides the AM and PL have been proposed for the anatomy of the ACL, however, these supposed anatomical structures are unlikely to be functionally discrete. In spite of this, from a macroscopic anatomical position, there is a large consensus that there are only the two bundles that are described in this paper [5, 60]. Nevertheless, all of this debate over the anatomy of a single ligament confirms that the ACL is evidently a geometrically complex structure and unlike any other ligament in the human body [5]. This is why graft tissues used to replace this ligament, in cases of injuries with extensive damage, can never successfully emulate the native function of the ACL [59].

4.2 - Biomechanics

The main function of the ACL is to prevent anterior translation of the tibia in relation to the femur, in fact, it is responsible for 87% of this effect at 30° of flexion and for 85% at 90° of flexion [7]. In fact, ACL-deficient knee have been shown to exhibit an anterior translation, of this type, four times greater than normal healthy knees [49]. This is due to the fact that the ACL is mostly oriented in the sagittal plane, consequently, anterior translation of the tibia leads to a greater separation of the attachments, which puts tension on the fibres and as a result, hinders the movement [5]. Besides this, the ACL also acts as an important secondary restraint to internal rotation, mainly near full extension. It also restrains varus/valgus stresses of the tibia, especially in cases of injury in the collateral ligaments [7, 49, 59].

When analysing the ACL into greater detail, it noticeable that its two bundles act differently during knee flexion. The AM bundle is taut at 90°of flexion while the PL bundle only reaches its maximum tightness near full knee extension [62]. The combined efforts of these two bundles give the ACL an ultimate tensile strength which is described in the literature to be within the 600 to 2300 N range [63].

4.3 – Sports-Related Injuries in the ACL

After understanding the biomechanical functions of the ACL and its importance in the movement of the knee joint, it becomes clear that the integrity and proper functioning of this ligament is incredibly important not only in day to day activities but also, and especially, for athletes. Sports that involve pivoting, cutting, jumping movements or sudden accelerations and decelerations put a lot of strain in this ligament, which is why ACL ruptures are one of the most common injuries sustained by athletes competing at the highest level [7].

When the injury occurs, a popping noise is usually heard, which is accompanied by discomfort and/or pain and within 4 hours, the knee normally swells up. There are several tests in order to determine the severity of the damage, however, the Lachman test and the pivot-shift test are two

of the most common, practical and sensitive methods. In the Lachman test (Figure 4.3), with the knee at 20° to 30° of flexion, the examiner performs an anterior force on the tibia while holding the femur, and anterior laxity is evaluated based on the degree of anterior translation in the tibia [64].

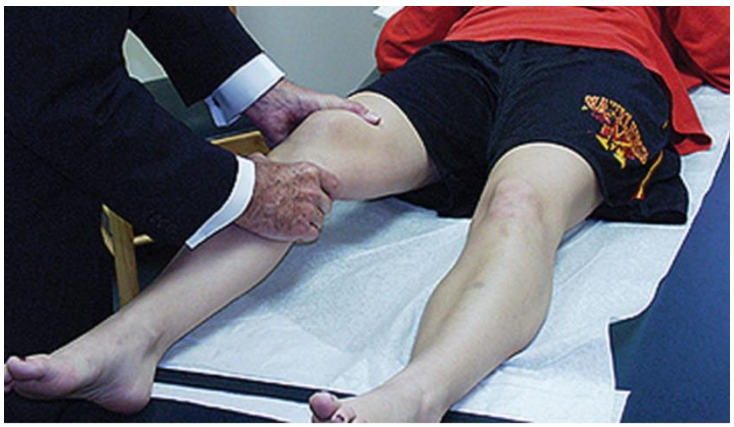

Figure 4.3 – A positive Lachman test [7].

The pivot shift test is performed on a fully extended knee and both a valgus stress and an axial load are applied, while the tibia is internally rotated, and the knee is flexed. In case of a torn ACL, the tibia will subluxate anteriorly and rotate internally (as shown in Figure 4.4) [7, 64].

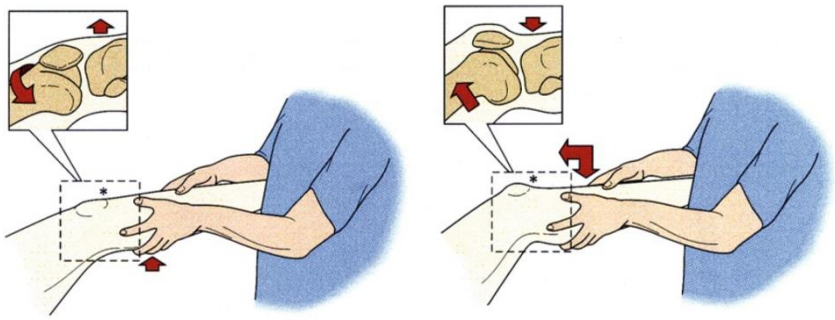

Figure 4.4 – The motions performed during a pivot-shift exam [7].

The ACL injury is classified as being either a partial or a complete tear of the ligament. A complete tear is usually characterized by an increased tibial translation of 5 mm or more when a Lachman test is performed and a positive pivot-shift test. When a Lachman test detects increased tibial translation, but it is smaller than 5 mm and coupled with a positive pivot-shift test, the patient is diagnosed with a partial tear where the ACL was able to retain some of its function [7].

After an ACL tear, the range of motion of the movement of flexion and extension of the knee is reduced. This reduction is attributed to the fact that the patient instinctively starts to reduce the activity of the quadriceps muscle at full extension, reducing the anterior force on the tibia which would be countered by the healthy ACL [65]. Besides this, damage to the ACL leads to severe instability in the knee, in fact, a complete ACL tear has been reported to cause long-term problems in the knee, including the early development of osteoarthritis [7, 8, 65]. Surgical reconstruction

of the ligament is not a perfect solution but without it the knee is far more unstable and prone to injury, the probability of damage to other structures of the joint such as the menisci and cartilages is increased and performance at a high level of sports activities worsens dramatically [64].

Video analysis, computer simulations, cadaveric studies and epidemiologic data have been essential tools in understanding what causes this type of injury, and despite all of this and the significant breakthroughs that this subject has seen in the last years, the mechanism behind ACL injuries remains somewhat unclear [66]. This is a consequence of the fact that realistic kinematic and kinetic data are incredibly difficult to obtain. Having healthy athletes perform movements and then measuring the strain on the ACL provides non-injury data, which fails to register the load magnitudes and the strain rates on the ligaments that compromise their integrity. Cadaveric studies cannot fully recreate the high loading rates and the intricate muscle activity involved in the stabilization of the knee joint [5, 67].

Most of the injuries to this ligament stem from the movements performed by the athletes without any type of collision or violent contact with, for example, an opponent. In fact, non-contact injuries account for around 70% of all injuries to the ACL [6]. Non-contact injuries occur when a person performs movements which produce forces or moments that apply excessive tension to the ACL.

ACL strain is often associated with anterior tibial translation, which is a consequence of the anterior shear force at the proximal end of the tibia, that the quadriceps muscle creates when creating knee moments [68]. In fact, a strong quadriceps contraction has already been linked to non-contact injuries to the ACL by DeMorat *et. al* [69]. Yet, more recent studies suggest that non-contact ACL injuries are caused by an intricate play of different forces and moments, and while an anterior shear force on the proximal end of the tibia is still considered one of the main causes of strain to the ACL, when it is combined with valgus moments of the knee, the resulting strain to this ligament is significantly larger [6, 8]. In fact, valgus alignment has been shown to greatly decrease the maximum axial force needed for injury to occur, supporting the theory that neutral limb alignment is important to prevent ACL injuries in movements such as the landing portion of a jump [70].

Besides valgus moments, varus and internal rotation moments have also been linked to higher ACL strain. However, it is important to stress that these moments can only significantly increase the load on the ACL when accompanied by strong anterior shear forces. In fact, even the valgus moment alone is incapable of rupturing the ACL unless the MCL is completely ruptured, since this ligament is the primary resistance to this moment [68].

The majority of the injuries to the ACL occur at full extension or at early flexion, this is due to the fact that in this range of motion, the contraction of the quadriceps muscle has been found to elicit higher strains on this ligament [66, 68]. Strong contractions of the quadriceps at or near full extension occur in movements of sudden deceleration, explaining why these are some of the most common moments of ACL injury [66].

The mechanism behind these injuries is so complex that in movements such as the landing portion of a jump, factors such as the initial ground contact with flat or near flat feet and increased

hip flexion have been shown to increase the likelihood of ACL injury. This is due to the fact that there is a decrease in the dampening capabilities of the leg to minimize the forces that reach the knee joint during intense physical activity [9].

The aim of this work is to study the damage on the ACL when the knee is performing some common movements that cause the injuries to the ligament. With this, the author hopes to shed some light on the mechanism behind this type of injury and the different movements that are involved in it, which is a critical step for developing and optimizing prevention strategies.

Chapter 5 – Continuum mechanics

Continuum mechanics refers to the study of the way materials act when subjected to different loading conditions. The continuum refers to an infinite amount of particles where every particle always has neighbouring particles in every direction. In this continuum, the position of a particle is defined by a vector with a specific set of coordinates and a combination of these vectors defines a body. In turn, the body has a reference configuration and multiple deformed configurations, which represent different deformation states [71].

When a particle is subjected to a load, a displacement occurs. The displacement vector in a continuum (X) from the reference configuration $P(t_0)$ to the deformation configuration $P(t)$ is given by the vector from $P(t_0)$ to $P(t)$, shown in the figure below as $\mathbf{u}$ $(\mathbf{X}, \mathbf{t})$ [71].

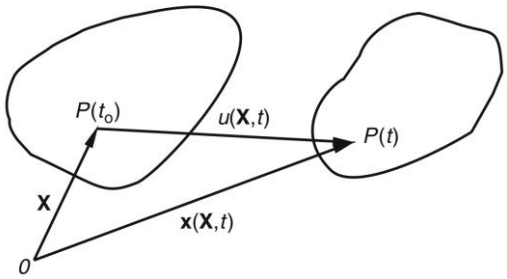

Figure 5.1 – Schematic representation of the displacement of a particle in a continuum [71].

As such, the displacement vector $\mathbf{u}$ is given by:

$$\mathbf{u} = \mathbf{x}(\mathbf{X}, \mathbf{t}) - \mathbf{X} \tag{5.1}$$

All the information relating to the local changes in lengths, volumes and angles derived from deformation caused by the imposition of a load are contained in the deformation gradient $\boldsymbol{F}$ [71]. Consider a material element $\mathrm{d}\mathbf{X}$ in its reference position deformed into a material element $\mathrm{d}x$, the relation between $\mathrm{d}\mathbf{X}$ and $\mathrm{d}x$ is given by:

$$\mathrm{d}x = x(\mathbf{X} + \mathrm{d}\mathbf{X}, \mathrm{t}) - x(\mathbf{X}, \mathrm{t}) = (\nabla x)\mathrm{d}\mathbf{X} \tag{5.2}$$

If the deformation gradient is defined as $\mathbf{F} = \nabla x$, the following equation is obtained:

$$\mathrm{d}x = \mathbf{F}\mathrm{d}\mathbf{X} \tag{5.3}$$

The deformation itself is usually considered to occur in two steps, a stretch step which stretches line elements to their final length and a rotation step, which orients them in the directions of the deformed configuration. This train of thought is called the polar decomposition theorem [72].

As such, the deformation gradient may be written as:

$$\mathbf{F} = \mathbf{RU} = \mathbf{VR} \tag{5.4}$$

Where $\mathbf{U}$ and $\mathbf{V}$ are symmetric matrices that define pure stretch deformations, called right and left stretch tensors, respectively [71].

With the polar decomposition theorem in mind, an alternative to the deformation gradient was introduced, the Right-Cauchy Green and the Left Cauchy Green [71].

The Right-Cauchy Green tensor is defined as:

$$\mathbf{C} = \mathbf{U}^2 = \mathbf{F}^\mathbf{T}\mathbf{F} \tag{5.5}$$

Whereas the Left-Cauchy Green is defined as:

$$\mathbf{B} = \boldsymbol{V}^2 = \mathbf{F}\mathbf{F}^\mathbf{T} \tag{5.6}$$

5.1 - Stress and Strain

The concepts of stress and strain are essential in continuum mechanics, as such, there are several ways to measure them.

Starting off with the strain, this is not a measurable quantity but rather a concept that was introduced to simplify analyses. In order to define the strain, there are several strain tensors, namely the Lagrangian strain tensor ($\mathbf{E}$):

$$\mathbf{E} = \frac{1}{2}\left(\mathbf{F}^\mathrm{T}.\mathbf{F} - \mathbf{I}\right) = \frac{1}{2}\mathbf{C} - \mathbf{I} \tag{5.7}$$

This tensor is usually used when analysing materials which present large strains and rotations [71, 73].

Besides this, the Eulerian strain tensor (**e**) is also used in the measuring of strains:

$$\mathbf{e} = \frac{1}{2}\left(\mathbf{I} - \mathbf{F}\mathbf{F}^{\mathrm{T}}\right) \tag{5.8}$$

It has a similar significance to the Lagrangian strain tensor and is used in similar situations. The main difference between the two is the fact that the Eulerian strain tensor allows to compute the strain of an infinitesimal line element after deformation [74].

Regarding the stress, before considering this concept, it is important to define the traction vector. This is a vector which represents the force being applied to a surface per unit of area of deformed solid:

$$\mathbf{t_n} = \lim_{dS \to 0} \frac{df_i}{dS^*} \tag{5.9}$$

In this equation, dS^* stands for a small element of area on a plane with a normal vector **n** subjected to a resultant force df_i. This vector is unique due to the fact that it needs to be associated with its normal vector **n** for it to be meaningful, as there is an infinite amount of traction vectors for each of the infinite cutting planes imaginable on the point which is being subjected to the applied force [73]. As such, it can be represented as:

$$\mathbf{t} = \mathbf{t}(x, t, \mathbf{n}) \tag{5.10}$$

Which can be defined by the linear transformation shown below:

$$\mathbf{t}(x, t, \mathbf{n}) = \boldsymbol{\sigma}^T(x, t).\,\mathbf{n} \tag{5.11}$$

Where **σ** is called the Cauchy Stress Tensor [75].

In some situations, it is more suitable to formulate motion equations with respect to the undeformed configuration instead of the deformed configuration. For this purpose, the first and second Piola-Kirchhoff stress tensors were defined. Since deformation can be described with the deformation gradient and with $\mathrm{J} = \det \mathbf{F}$, the Kirchhoff stress can be defined from the Cauchy stress by the equation below [74].

$$\boldsymbol{\tau} = \mathrm{J}\boldsymbol{\sigma} \tag{5.12}$$

In contrast to the Cauchy traction vector $\mathbf{t}$, which represents the actual force per unit area which acts on the deformed solid, the nominal Piola-Kirchhoff traction vector $\mathbf{T}(\mathbf{X}, t, \mathbf{N})$ has no real physical significance in describing the intensity of the force. It can be considered as the force acting on an element in the deformed configuration per area of the matching element in the undeformed configuration:

$$\mathbf{T} = \frac{df}{dS} \tag{5.13}$$

The First Piola-Kirchhoff stress tensor $\mathbf{P}$ can be defined as:

$$\mathbf{P} = \mathrm{J}\boldsymbol{\sigma}\mathbf{F}^{-1} \tag{5.14}$$

While the Cauchy stress is symmetric, the same does not apply to the First Piola-Kirchhoff stress tensor, which limits its usage. Due to this fact, the Second Piola-Kirchhoff stress tensor was formulated [74]:

$$\boldsymbol{\Sigma} = \mathrm{J}\boldsymbol{\sigma}\mathbf{F}^{-\mathrm{T}}.\mathbf{F}^{-\mathbf{1}} \tag{5.15}$$

5.2 - Hyperelasticity

A material is considered elastic if it has both of the following properties: It displays the stress-strain relation, meaning that the stress at one of its specific points depends only on the measure of present strain at that point, and its Cauchy stress field is always symmetric [76].

Within the elastic materials, one particular subgroup can be highlighted, the hyperelastic materials. In these, the work performed by the stresses it is subjected to during deformation are exclusively dependant on the initial and final configurations. As such, these materials are said to be path-independent [77]. Due to this particularity, it is possible to define a Helmholtz free-energy function Ψ, which is referred to as the stored energy function where $\Psi = \Psi(\mathbf{F})$. With it, the Piola-Kirschhoff tensor ($\mathbf{S}$) presented in the previous section can be defined as:

$$\mathbf{S} = \frac{\partial \Psi(\mathbf{F})}{\partial \mathbf{F}} \tag{5.16}$$

Which, combined with the symmetric Cauchy stress tensor where $\boldsymbol{\sigma} = \mathrm{J}^{-\mathbf{1}}\mathbf{P}\mathbf{F}^{\mathrm{T}}$, results in the following equation:

$$\boldsymbol{\sigma} = \mathrm{J}^{-1}\mathbf{F}\left(\frac{\partial\Psi(\mathbf{F})}{\partial\mathbf{F}}\right)^{\mathrm{T}} \tag{5.17}$$

And considering the right Cauchy-Green tensor the following equation is obtained [78]:

$$\boldsymbol{\sigma} = 2\mathrm{J}^{-1}\mathbf{F}\left(\frac{\partial\Psi(\mathbf{C})}{\partial\mathbf{C}}\right)\mathbf{F}^{\mathrm{T}} \tag{5.18}$$

5.3 - Isotropic Hyperelasticity

Within the hyperelastic materials, it is possible to restrict the stored energy function by a property named isotropy. This states that the response of the material to stress-strain situations is the same in all directions. In this case, the relationship between Ψ and $\mathbf{C}$ is independent on the material axis. As such, Ψ becomes a function of the invariants of $\mathbf{C}$ [78]. This is shown in following equation:

$$\Psi(\mathbf{C}, \mathbf{X}) = \Psi(\mathrm{I}_1\mathrm{I}_2\mathrm{I}_3\mathbf{X}) \tag{5.19}$$

Where I_1, I_2 and I_3 are defined as:

$$\begin{aligned} \mathrm{I}_1(\mathbf{C}) &= \mathrm{trace}(\mathbf{C}) \\ \mathrm{I}_2(\mathbf{C}) &= \frac{1}{2}(\mathrm{I}_1^2\mathbf{C}\colon\mathbf{C}) \\ \mathrm{I}_3(\mathbf{C}) &= \det(\mathbf{C}) = \mathrm{J}^2 \end{aligned} \tag{5.20}$$

5.3.1 - Transverse isotropic materials

Many biological tissues, including ligaments, are made up of one or more families of fibres embedded in a matrix material [79].

These materials are regarded as transverse isotropic, a specific type of materials which are quite heterogenous. They are mechanically regarded as anisotropic and possess strong directional properties, in fact, they are isotropic along two of the main axes [80].

The anisotropic properties that these materials present are attributed to the presence of the fibres while the matrix behaves as an isotropic material. A composite material of this sort with a single family of fibres demonstrates different mechanical properties along the direction of the fibres, where its stiffness is significantly larger than in orthogonal directions. This direction is

referred to as the preferred direction which is referenced, in the reference configuration, by a unit vector field $\mathbf{a}_0(\mathbf{X}), |\mathbf{a}_0| = 1$. In the deformed configuration a new direction is defined by the unit vector field $\mathbf{a}(\mathrm{x}, \mathrm{t}), |\mathbf{a}| = 1$ [78]. These two can be related in the following equation:

$$\lambda \mathbf{a} = \mathrm{F}\mathbf{a}_0 \tag{5.21}$$

Where λ represents the stretch tensor. The Helmholtz free energy function, assuming hyperelasticity, can be defined as the tensor product $\mathbf{a}_0 \otimes \mathbf{a}_0$ and expressed as a function of the Cauchy-Green tensor $\mathbf{C}$:

$$\Psi = \Psi(\mathbf{C}, \mathbf{a}_0 \otimes \mathbf{a}_0) \tag{5.22}$$

In order to form the integrity bases of the tensors $\mathbf{C}$ and $\mathbf{a}_0 \otimes \mathbf{a}_0$ and to satisfy their relation, two new scalars are required beyond the first three $(\mathrm{I}_1, \mathrm{I}_2, \mathrm{I}_3)$ which were already defined in the previous section. These are called the pseudo-invariants of $\mathbf{C}$ and $\mathbf{a}_0 \otimes \mathbf{a}_0$ and come directly from the anisotropy and contribute to the free energy. They are shown below as I_4 and I_5 [78]:

$$\begin{aligned} \mathrm{I}_4(\mathbf{C}, \boldsymbol{a_0}) &= \mathbf{a}_0 . \mathbf{C}\mathbf{a}_0 = \lambda^2 \\ \mathrm{I}_5(\mathbf{C}, \boldsymbol{a_0}) &= \mathbf{a}_0 . \mathbf{C}^2\mathbf{a}_0 \end{aligned} \tag{5.23}$$

Chapter 6 - Finite Element Method

When a load or a force is applied to a solid, it is said to be stressed. These stresses cause deformations or relative displacements in the solid, which are in turn called strains. Solid mechanics handle the relation between these stresses and strains that act on a solid, as well as, the relation between the strains and displacements [81].

Solids act according to their material properties. They can be classified as elastic, if the deformation that the loading imposes on them is completely reversible when the load is removed. In opposition, materials which present permanent deformation after the load is removed are classified as plastic [81]. Besides this, solids may also be classified as isotropic or anisotropic, depending on their material properties. In anisotropic materials, the deformation caused by a load applied in a specific direction is different from the deformation that the same load with the same of force causes when applied in a different direction [82]. In these cases, the material properties are dependent on the direction in which the force is applied. This leads to a tremendous amount of material constants that need to be specified to describe such materials, therefore, in engineering problems, these materials are often dealt with by assuming isotropic behaviour to simplify the analysis. In isotropic materials, the material properties are independent from the direction of the force, this is the case in many engineering materials. For this case, only two independent material properties are required to fully describe the materials, the Young modulus and the Poisson ratio, which simplifies the process quite a bit [81, 82].

There are six independent stress components at a specific point of an elastic continuous 3D solid. These stress components are usually called stress tensors and can be written in a vector form as shown below:

$$\boldsymbol{\sigma} = \{\boldsymbol{\sigma}_{xx} \quad \boldsymbol{\sigma}_{yy} \quad \boldsymbol{\sigma}_{zz} \quad \boldsymbol{\sigma}_{xy} \quad \boldsymbol{\sigma}_{yz} \quad \boldsymbol{\sigma}_{zx}\}^{T} \tag{6.1}$$

Simultaneously, there are also three strain components which can be written in a vector form:

$$\boldsymbol{\varepsilon} = \{\boldsymbol{\varepsilon}_{xx} \quad \boldsymbol{\varepsilon}_{yy} \quad \boldsymbol{\varepsilon}_{zz} \quad \boldsymbol{\varepsilon}_{xy} \quad \boldsymbol{\varepsilon}_{yz} \quad \boldsymbol{\varepsilon}_{zx}\}^{T} \tag{6.2}$$

This strain vector ($\boldsymbol{\varepsilon}$) may also be written as:

$$\boldsymbol{\varepsilon} = \boldsymbol{L}\mathbf{u} \tag{6.3}$$

Where $\mathbf{u}$ is the displacement vector and $\boldsymbol{L}$ is a matrix of partial differential operators.

In isotropic behaviour, which is assumed in the model used for this work, the relation between the stress ($\boldsymbol{\sigma}$) and strain in a 3D solid is given by the constitutive equation called Hooke's law presented below:

$$\boldsymbol{\sigma} = \boldsymbol{c}\,\boldsymbol{\varepsilon} \tag{6.4}$$

$\boldsymbol{c}$ is a matrix called constitutive matrix and is made up of material constants obtained from experimental data [81].

The partial differential system equations that rule a physical phenomenon are made up of strong form system equations. However, determining exact solutions from strong form system equations is often tremendously difficult to manage when dealing with complex engineering problems. Therefore, the weak form system equations are preferable since they lead to discrete system equations capable of providing accurate results [81]. In this work, the Galerkin weak form is the method used to obtain these discrete system equations. It is a variational principle based on energy minimization, the real solution minimizes the Langrangian functional which can be represented as:

$$L = T - U + W_{\mathrm{f}} \tag{6.5}$$

Where T represents the kinetic energy:

$$T = \frac{1}{2}\int_{\Omega} \rho\, \dot{\mathbf{u}}^{\mathrm{T}}\dot{\mathbf{u}}\, \mathrm{d}\boldsymbol{\Omega} \tag{6.6}$$

$\boldsymbol{\Omega}$ is the domain which describes the body, $\dot{\mathbf{u}}$ is the first derivative of the displacement and ρ is the density of the body.

The U represents the strain energy and is defined as:

$$U = \frac{1}{2}\int_{\Omega} \boldsymbol{\varepsilon}^{\mathrm{T}}\boldsymbol{\sigma}\, \mathrm{d}\boldsymbol{\Omega} \tag{6.7}$$

Finally, the W_{f} represents the work performed by the external forces and is expressed as:

$$W_{\mathrm{f}} = \int_{\Omega} \mathbf{u}^{\mathrm{T}} \boldsymbol{b} \, \mathrm{d}\boldsymbol{\Omega} + \int_{\Gamma_{\mathrm{t}}} \mathbf{u}^{\mathrm{T}} \, \bar{\boldsymbol{t}} \, \mathrm{d}\boldsymbol{\Gamma} \tag{6.8}$$

With $\mathbf{u}$ being the displacement, $\boldsymbol{b}$ the body force vector and $\bar{\boldsymbol{t}}$ the traction on the natural boundary where the external forces are applied [81].

As such, the Galerkin weak form can be represented as:

$$L = \frac{1}{2}\int_{\Omega} \rho \, \dot{\mathbf{u}}^{\mathrm{T}} \dot{\mathbf{u}} \, \mathrm{d}\boldsymbol{\Omega} - \frac{1}{2}\int_{\Omega} \boldsymbol{\varepsilon}^{\mathrm{T}} \boldsymbol{\sigma} \, \mathrm{d}\boldsymbol{\Omega} + \int_{\Omega} \mathbf{u}^{\mathrm{T}} \boldsymbol{b} \, \mathrm{d}\boldsymbol{\Omega} + \int_{\Gamma_{\mathrm{t}}} \mathbf{u}^{\mathrm{T}} \, \bar{\boldsymbol{t}} \, \mathrm{d}\boldsymbol{\Gamma} \tag{6.9}$$

Disregarding the dynamic part of the equation, which is the kinetic energy variation, and after some rearrangements, the result is the equation below:

$$\int_{\Omega} \delta\boldsymbol{\varepsilon}^{\mathrm{T}} \boldsymbol{\sigma} \, \mathrm{d}\boldsymbol{\Omega} - \int_{\Omega} \delta\mathbf{u}^{\mathrm{T}} \boldsymbol{b} \, \mathrm{d}\boldsymbol{\Omega} - \int_{\Gamma_{\mathrm{t}}} \delta\mathbf{u}^{\mathrm{T}} \bar{\boldsymbol{t}} \, \mathrm{d}\boldsymbol{\Gamma} = 0 \tag{6.10}$$

Taking the first term of the previous equation and applying Hooke's law for isotropic behaviour, which was mentioned at the beginning of this chapter, it is possible to obtain the following:

$$\begin{aligned}
\int_{\Omega} \delta\boldsymbol{\varepsilon}^{\mathrm{T}} \boldsymbol{\sigma} \, \mathrm{d}\boldsymbol{\Omega} &= \int_{\Omega} (\delta \boldsymbol{L}\mathbf{u})^{T} \boldsymbol{c} \, (\boldsymbol{L}\mathbf{u}) \mathrm{d}\boldsymbol{\Omega} = \int_{\Omega} (\boldsymbol{L}\boldsymbol{H}\delta\mathbf{u}_{\mathrm{s}})^{T} \boldsymbol{c} \, (\boldsymbol{L}\boldsymbol{H}\mathbf{u}_{\mathrm{s}}) \mathrm{d}\boldsymbol{\Omega} \\
&= \int_{\Omega} \delta\mathbf{u}_{\mathrm{s}}{}^{T} \boldsymbol{B}^{T} \boldsymbol{c} \, \boldsymbol{B} \, \mathbf{u}_{\mathrm{s}} \, \mathrm{d}\boldsymbol{\Omega} = \delta\mathbf{u}^{\mathrm{T}} \int_{\Omega} \boldsymbol{B}^{T} \boldsymbol{c} \, \boldsymbol{B} \, \mathrm{d}\boldsymbol{\Omega} \, \boldsymbol{u} \\
&= \delta\mathbf{u}^{T} \sum_{\boldsymbol{I}=1}^{\boldsymbol{Q}} \left[\widehat{\omega}_{\boldsymbol{I}} \, \boldsymbol{B}_{\boldsymbol{I}}^{T} \boldsymbol{c} \, \boldsymbol{B}_{\boldsymbol{I}}\right]\mathbf{u} = \delta\mathbf{u}^{T} \sum_{\boldsymbol{I}=1}^{\boldsymbol{Q}} [\boldsymbol{K}_{\boldsymbol{I}}]\mathbf{u} = \delta\mathbf{u}^{T} \boldsymbol{K} \, \mathbf{u}
\end{aligned} \tag{6.11}$$

Where $\widehat{\omega}_{\boldsymbol{I}}$ is the integration weight, $\boldsymbol{B}_{\boldsymbol{I}}$ is the deformability matrix for the n nodes that make up the element, $\boldsymbol{H}$ is the interpolation function matrix and $\boldsymbol{K}_{\boldsymbol{I}}$ is the local stiffness matrix, which is ultimately combined with all the other $\boldsymbol{K}_{\boldsymbol{I}}$, determined for each integration point, and together these will form the global stiffness matrix $\boldsymbol{K}$.

From the second and third terms of equation (6.10), respectively, it is possible to obtain the following simplified expressions:

$$\begin{aligned}\int_{\Omega} \delta\mathbf{u}^{\mathrm{T}}\boldsymbol{b}\,\mathrm{d}\boldsymbol{\Omega} &= \int_{\Omega} (\boldsymbol{H}\delta\mathbf{u}_{\mathrm{s}})^{T}\boldsymbol{b}\,\mathrm{d}\boldsymbol{\Omega} = \delta\mathbf{u}^{\mathrm{T}}\int_{\Omega}\boldsymbol{H}^{T}\boldsymbol{b}\,\mathrm{d}\boldsymbol{\Omega} = \delta\mathbf{u}^{\mathrm{T}}\sum_{\boldsymbol{I}=1}^{\boldsymbol{Q}}[\widehat{\omega}_{I}\,\boldsymbol{H}_{I}^{T}\boldsymbol{b}] \\ &= \delta\mathbf{u}^{T}\sum_{\boldsymbol{I}=1}^{Q}[\boldsymbol{f}_{bI}] = \delta\mathbf{u}^{\mathrm{T}}\boldsymbol{f}_{b}\end{aligned} \tag{6.12}$$

$$\begin{aligned}\int_{\Gamma_{\mathrm{t}}} \delta\mathbf{u}^{\mathrm{T}}\bar{\boldsymbol{t}}\,\mathrm{d}\boldsymbol{\Gamma} &= \int_{\Omega} (\boldsymbol{H}\delta\mathbf{u}_{\mathrm{s}})^{T}\bar{\boldsymbol{t}}\,\mathrm{d}\boldsymbol{\Gamma} = \delta\mathbf{u}^{\mathrm{T}}\int_{\Omega}\boldsymbol{H}^{T}\bar{\boldsymbol{t}}\mathrm{d}\boldsymbol{\Gamma} = \delta\mathbf{u}^{\mathrm{T}}\sum_{\boldsymbol{I}=1}^{Q^{*}}[\widehat{\omega}_{I}{}^{*}\boldsymbol{H}_{I}^{T}\bar{\boldsymbol{t}}] \\ &= \delta\mathbf{u}^{T}\sum_{I=1}^{Q^{*}}[\boldsymbol{f}_{tI}] = \delta\mathbf{u}^{T}\boldsymbol{f}_{t}\end{aligned} \tag{6.13}$$

Where $\boldsymbol{f}_{b}$ is the global body force vector and $\boldsymbol{f}_{t}$ is the global external force vector. Since the magnitude of the external force is usually much higher than the one for the body force vector, the effect of the body can be neglected. The resulting equilibrium equation is shown below:

$$\delta\mathbf{u}^{\mathrm{T}}\boldsymbol{K}\,\mathbf{u} - \delta\mathbf{u}^{\mathrm{T}}\boldsymbol{f}_{t} = 0 \qquad \rightarrow \qquad \boldsymbol{K}\,\mathbf{u} = \boldsymbol{f}_{t} \tag{6.14}$$

From this last equation, it is possible to obtain the displacement field $\mathbf{u}$ [83].

The finite element method (FEM) is a numerical method which has been used numerous times to study the biomechanics of the knee joint [30]. This method was created in the later 1950's and early 1960's, only a short while after the development of the first computer. In fact, its origins date back to 1956, where Turner *et. al* [84]. came up with a numerical method for solving complex structural problems which would be used as the starting point for the development of the FEM [85]. The first application of this method to the area of biomechanics was in 1972, and since then it has become a popular and effective tool used in several areas of engineering [30].

In the FEM, the domain is discretized into finite elements which are connected by nodes, creating a mesh where every element is either directly or indirectly connected [83]. This way, complex geometries are represented by a set of small elements (Figure 6.1). These geometries are approximated by straight lines or flat surfaces, this implies that, the accuracy of a curved part, for example, is dependent on the number of elements that make up the mesh that is obtained from it. After subdividing the problem domain, linear functions are developed for each element. These equations of each of the individual elements are assembled and from them, the equations that represent the global system are obtained. After solving these global equations, the FEM can

determine quantities of interest, which may be, for example, the strains or stresses felt at different points of the mesh [82, 86].

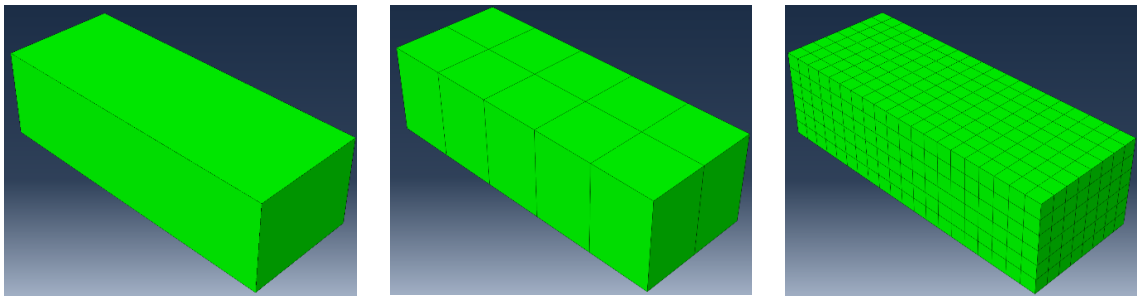

Figure 6.1 – Discretization of the initial domain (left) into two different meshes: one with a small number of elements and nodes (middle) and one with a large number of elements and nodes (right).

As it was previously mentioned, in order to obtain the discrete equation system, weak form system equations are used. However, it is impossible to use analytical integration when solving the weak form, therefore, it is necessary to resort to numerical integration. Since the integrals used in the FEM are typically polynomial, the Gauss quadrature is often employed for this purpose [86]. In the Gauss quadrature, the domain is divided into a grid, which is converted into an isoparametric grid, of natural coordinates, and then, each cell of this grid is given their respective integration points, as shown in Figure 6.2. With these, a correspondence can be established between the cartesian and the parent coordinates, which allows for the specification of shape functions in natural coordinates. From these shape functions, it is possible to obtain the element properties established in the global coordinate system [82, 87].

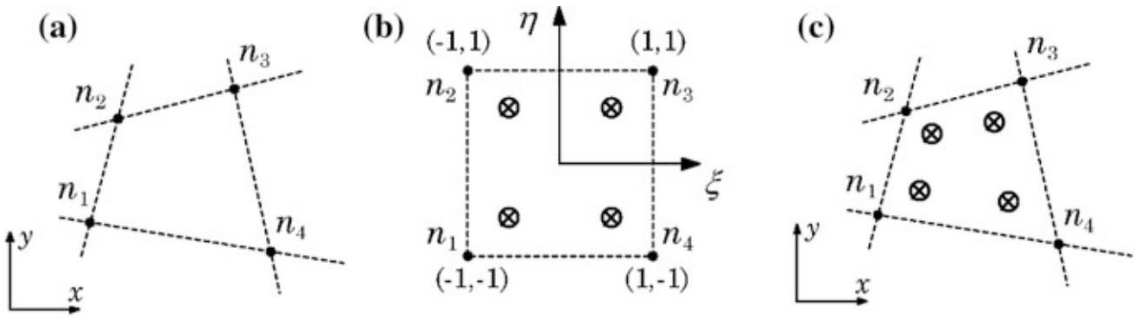

Figure 6.2 – (a) initial domain divided into a grid; (b) conversion to isoparametric grid and attribution of integration points; (c) Return to initial shape [81].

6.1 - Geometric Model

The geometric model is the basis for performing simulations using the FEM, and, in order to obtain reliable results, the chosen model must accurately represent the anatomical structures that are being studied. When the structure and properties of the geometric model are as similar as possible to the real structure, it becomes safe to extrapolate the obtained results to real life behaviour [86]. Having said this, the steps involved in the creation of a model to precisely mimic an incredibly complex structure as the human knee joint require a tremendous amount of time to perform. Nowadays there are a vast number of knee joint models which have already been created and described in the literature [3, 30, 88, 89].

In this work, the geometry of the knee joint which was used was based on a widely used open source model, with a solid degree of detail, obtained from the Open Knee project. This way, several lengthy developmental steps were circumvented.

The Open Knee is a model of the tibiofemoral joint with all of the structures that are involved in this joint, which were previously described in this paper: the femur (only the distal portion),the tibia (proximal portion), the articular cartilages, both the medial and lateral menisci and the 4 main ligaments of the joint (ACL, PCL,MCL and LCL). The model was based on the anatomical and mechanical data obtained from the right knee of the cadaver of a 70 year old female donor with a height of 1.68 m and a weight of 77.1 kg [90]. It is a freely accessible finite element model which has served as the basis for many studies using finite element models of the knee in the last years [91-94].

Although this model was chosen due to its convenience and level of detail, it is also important to note that it is not without its limitations. The main limitations are the absence of the patellofemoral joint and its main structures besides the femur, such as the patella and the patellar tendon. It also lacks the fibula bone and the joint capsule of the knee, as well as many of the soft tissues around the joint such as the skin and muscles [89]. However, since the aim of this work is to study the influence of the movement of the knee on the ACL, these shortcomings are of little importance, since their contribution to the movement of the joint is close to none. The absence of the fibula bone, for example, is the reason why the LCL is not distally connected to any surface and simply follows the movement of the tibia, which in itself is no major issue since the fibula would be connected to the tibia, therefore, its movement would be the same.

The Open Knee consists of an Abaqus (Simulia, Providence, USA) input file with the entire knee model previously assembled and meshed. The model which is obtained is represented in the figure below.

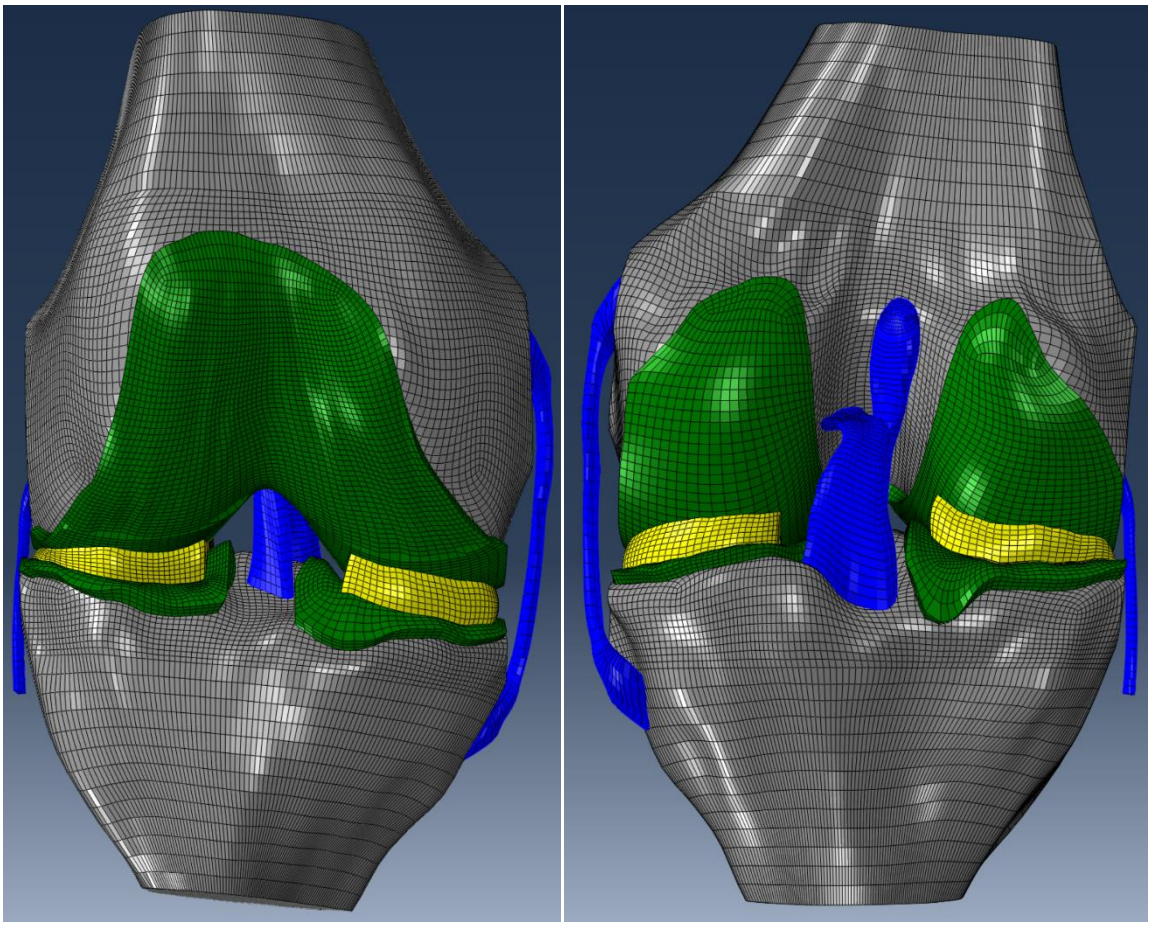

Figure 6.3 – Mesh of the entire knee model used in this work. Each group of anatomical structures is represented in different colours: Bones (grey), ligaments (blue), articular cartilages (green) and menisci (yellow).

In order to improve the reliability of the results which were obtained in this work and the stability of the model, some modifications were performed to the pre-existing model, acquired from the Open Knee Project, using the Abaqus input file.

The first modification was the introduction of 3D vertical fibres in the ligaments to simulate the collagen fibres that make up these structures since these are the main structures of the ligaments of the human knee and therefore, their absence would have a significant impact in the tension values that would be obtained in these structures. The fibres that were added are shown in the figure below.

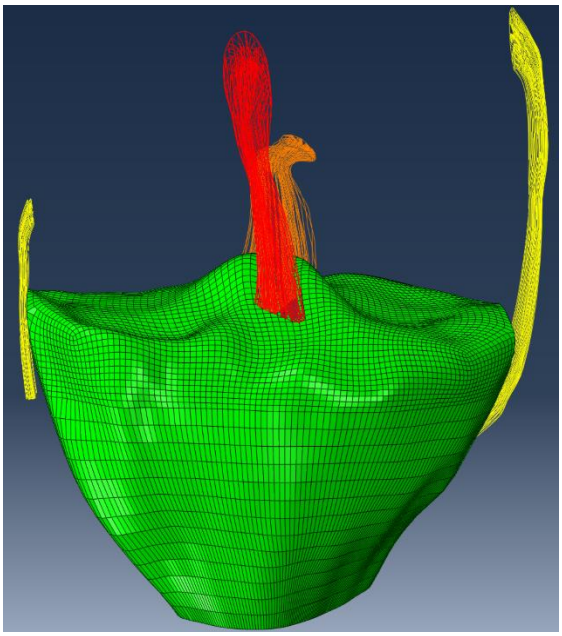

Figure 6.4 – Front view of the fibres of the knee ligaments: ACL (red), PCL (orange), collateral ligaments (yellow).

In the original model, the menisci are immobile and fixed to the tibial cartilages using a "tie" function. In reality, as was previously mentioned in Section 3.1.1.2, the menisci have some mobility which plays an important role in their ability to act as efficient load bearing structures in a dynamic knee joint.

In order to account for this, the "tie" function that fixed the menisci to the tibial cartilages was removed and switched with contact pairs between the menisci and the articular cartilages of the two bones. This way, the menisci were free to move around. However, by freeing the menisci from the tibial cartilages, the simulation started to become unstable due to the movement of these structures which were now completely loose and moved violently. To counter this effect, some springs and some elastic bars were added to the menisci, which fixed them to the tibial cartilages but allowed for some small movements to be performed so that these structures could adjust their position along with the movement of the joint. These springs and elastic bars are shown in Figure 6.5.

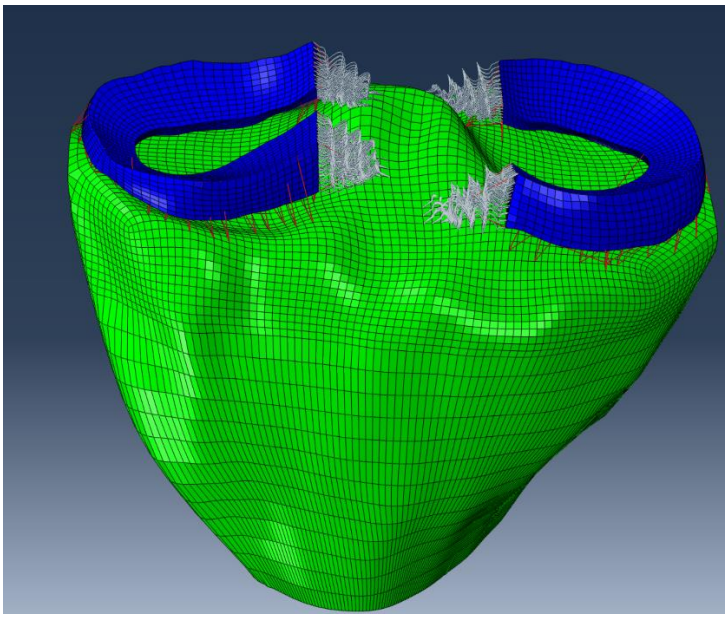

Figure 6.5 – Elastic bars (red) and springs (white) that were added to the model to stabilize the menisci.

This model was subjected to a simple test to evaluate its stability and accuracy and was used to study the kinematics of the knee joint in order to understand the different movements that may be imposed on it.

The implementation of the UMAT is a strenuous process involving several attempts and adjustments to some parameters, as such, the geometric model had to be simplified in order to reduce the computational power needed to complete each simulation and, consequently, simplify the analysis of the ACL injury, otherwise, it would be impossible to obtain the necessary results in this work within the stipulated time period.

In this simplified version (Figure 6.6), the model consisted only of the femur and tibia and the ACL between them. And although the model complexity was reduced, some measures were taken in order to avoid, as much as possible the resulting decrease in the reliability of the results. Firstly, the kinematics of all of the movements which were tested in this work were previously obtained from the initial and more complete model and only then were they applied to the simplified model with the UMAT in order to obtain the results which are shown in Section 7.3. Besides this, the ACL geometry was improved to increase the reliability of the results, since this is the main structure of interest in this work. Instead of a single, somewhat uniform structure, the ligament was divided into two bundles in order to more closely emulate its structure, as shown in Figure 6.7.

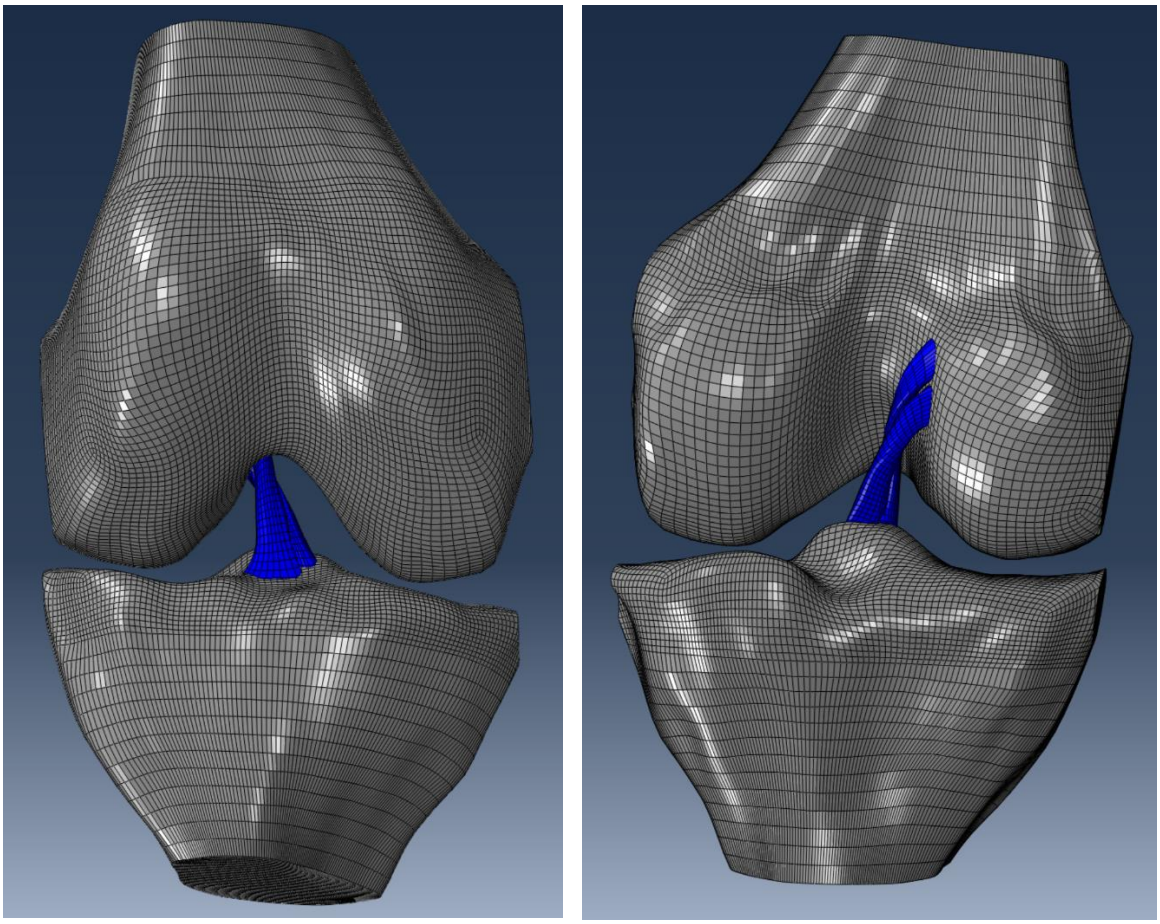

Figure 6.6 – Simplified model used in this work for the incorporation of the damage parameter. Left – Anterior view; Right – Posterior view.

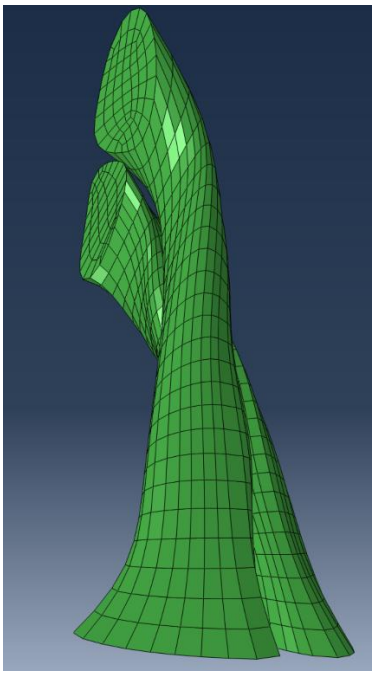

Figure 6.7 – Improved geometry of the ACL used in the simplified model.

6.2 – Material Properties

In order to create a finite element model of the knee, it is necessary to define the material properties of each of the main anatomical structures that were included.

The tibia and the femur are the only two bones which were included. Since the stiffness of the bones is significantly higher than that of the other structures that were included, which are soft tissues, these were modelled as rigid bodies. Bones are often modelled like this because, this way, it is possible to drastically reduce the computational cost of the simulation with almost no reduction in the reliability of the results [88].

In the first model, the articular cartilage and the menisci were modelled as linear elastic isotropic materials, an approach that has been used in several studies and that limits the computational cost and numerical difficulties [95].

Regarding the ligaments, these are made up of fibres and a support matrix to these fibres. The fibres are the elements that support the traction stresses while the matrix only serves to support the fibres and keep their cohesion. In both cases, the Neo-Hook hyperelastic model was used and a set of mechanical properties was attributed to all ligament fibres (C10=280 MPa and D1=0.32), while a different set of mechanical properties was attributed to the support matrix (C10=0.1 MPa and D1=0.3).

The mechanical properties of all the structures that were previously mentioned are shown in the table below.

Table 6.1 – Mechanical properties of the main components of the knee joint that were included in the finite element model.

Anatomical Structure	Young's Modulus (MPa)	Poisson Coefficient	Reference
Cartilage	5	0.46	[28, 96, 97]
Meniscus	59	0.45	[97-99]

Regarding the model with the UMAT, which was used to analyse the numerical damage, the material properties of the ligament were also changed. Instead of applying a simple Neo-Hook hyperelastic model with different properties for the fibres and extracellular matrix, a different approach was used and a new constitutive model was employed in order to take these differences into account. As such, in this model, the ACL was defined using a constitutive model which was developed specifically for transversely isotropic materials, such as ligaments, called the Holzapfel-Gasser-Ogden (HGO) model.

In this model, the following relation is established for the strain energy density of fibres (Ψ_{fib}):

$$\Psi_{fib}(\mathbf{C}, \mathbf{a}_0) = \frac{k_1}{2k_2}[e^{(k_2(I_4-1)^2)} - 1] \tag{6.15}$$

Where $k_1 > 0$ is a material parameter with the dimension of stress and $k_2 > 0$ is a dimensionless material parameters, both refer to the properties of the collagen fibres. The $\mathbf{a}_0$ vector defines the direction of the fibre families (which can be either a single fibre family or two families) in the reference configuration [100, 101]. It was obtained, for each of the fibres that were incorporated in the model, using a Matlab routine (see appendix) which created a vector, at the centroid of each of the 3000 elements that made up the ACL geometry in this model, with the direction of node 1 to node 4 (Figure 6.8). The constants k_1 and k_2 that were used are shown in Table 6.2.

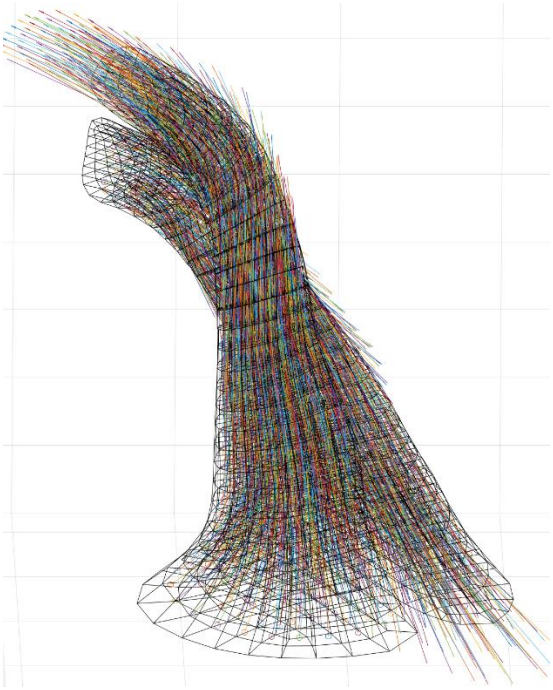

Figure 6.8 – Fibre directions obtained with the Matlab routine.

As was previously said, in order to implement the HGO material model, a user material subroutine was defined, based on the subroutine developed by Ferreira J.P.S. *et al.*, 2017 [102].

For the sake of more accurately representing the ACL behaviour during the motions which were tested, a numerical damage parameter was added to the constitutive model, using this UMAT. This way, it became possible to identify where the damage to the collagen fibres is more likely to occur, when it is expected to start during a specific motion and its extent. For this purpose, an internal state variable, as presented in Calvo *et al.*, 2007 [103], was included in the material model.

With it, the strain energy function (U) is represented as what is shown in the following equation:

$$U = (1 - D_m)U_I\big(1 - D_f\big)U_f + U_J \tag{6.16}$$

Where U_I and U_f are the effective strain energy function. While D_m and D_f are damage variables of the matrix and fibres, respectively.

The following equation shows the relation between the damage variables and the material, D_K:

$$D_K = \begin{cases} 0 & if \quad \Xi_{kt} < C \\ \xi^{\,2}[1 - \beta_{\,k}(\xi^{\,2} - 1)] & if \quad \Xi^0_{min} \le \Xi_{kt} \le \Xi^0_{max} \\ 1 & if \quad \Xi_{kt} > \Xi^0_{max} \end{cases} \tag{6.17}$$

Where $\mathrm{k} = [\mathrm{m}, \mathrm{f}]$, $\xi = (\Xi_{kt} - \Xi^0_{max})/(\Xi^0_{max} - \Xi^0_{min})$ is a dimensionless variable, Ξ^0_{min} and Ξ^0_{max} are variables which indicate the strain energies at initial and total damage, respectively. This means that if the strain energy value at a specific location exceeds the threshold set by the Ξ^0_{min}, the model starts accumulating damage and, at that location, the ligament starts to gradually lose its rigidity until the strain energy reaches the value set by Ξ^0_{max}, where the damage is considered total. Consequently, at that specific location, the ligament completely loses rigidity. The value of the strain energy $\beta_{\,k}$ is an exponential parameter collected from experimental data. All of these parameters, as well as the material parameters, referring to the HGO model, were adjusted using the experimental data from Paschos N.K. *et al.*, 2010 [104]. The resulting parameters are shown in the table below.

Table 6.2 – Material and damage parameters used to implement the HGO material model coupled with a damage parameter.

Material Parameters	**Damage Parameters**
$k1 = 7.00$ MPa	$\Xi^0_{min} = 1.00$ J
$k2 = 1.00$	$\Xi^0_{max} = 3.42$ J

The damage parameter was only applied to the fibres of the ACL, which are responsible for most of its structural integrity, therefore, the matrix was left without damage in the simulations in order to improve their stability.

Chapter 7 – Results and Discussion

7.1 - Knee Kinematics

After the modifications to the original Open Knee model, a numerical simulation was performed in order to evaluate the kinematics of the knee joint. The model was subjected to the natural rotation of the knee joint when the knee is flexed. A flexion of 90 degrees was imposed to the femur. The simulation ran until around 47 degrees of flexion where it was aborted due to an inability to achieve force equilibrium. However, since the aim of this work is to study the ACL injury, 47 degrees of flexion are enough for this purpose since, as was previously mentioned in Chapter 4.3, these injuries occur with the knee at full or near full extension.

With the results that were obtained, the maximum principal stress was calculated at 4 different nodes in different areas of the ACL, which were numbered as shown in Figure 7.1, to measure the stresses to which this ligament was exposed.

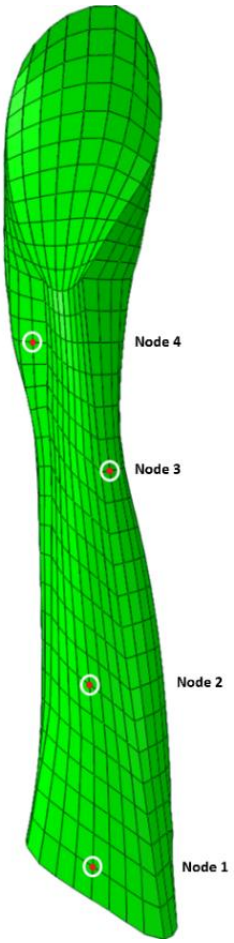

Figure 7.1 – Nodes from the ACL that were chosen for the evaluation of the stresses that were applied to this ligament (red dots surrounded by white circles).

The graphs that were obtained for each node are shown below.

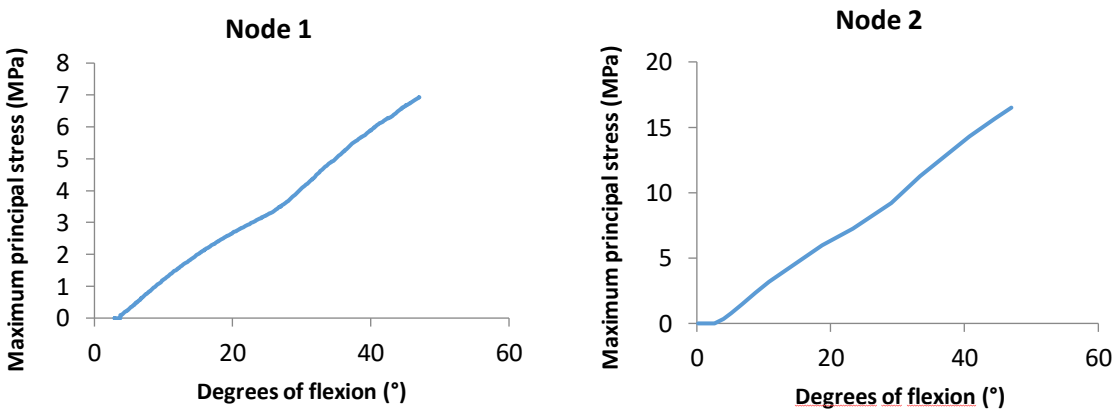

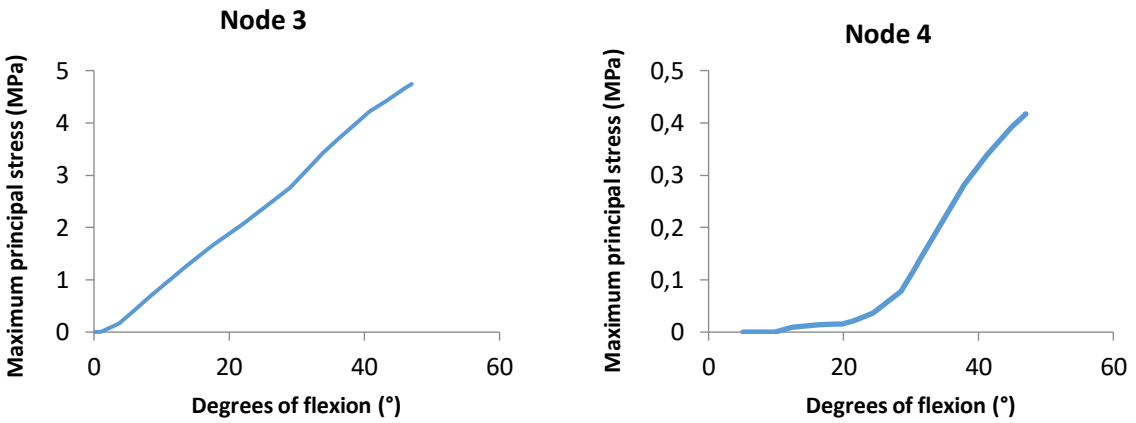

Figure 7.2 – Graphs obtained for the maximum principal stress applied to each of the chosen nodes plotted with the increase of the degree of knee flexion.

The graphs show that the maximum principal stress on the ACL is quite different depending on the location from where it is calculated. It is higher close to the middle portion of the ligament, especially in the region of Node 2 where it reached over 16 MPa. This is according to what can be found in the literature, the stresses that act on the ACL are not uniformly distributed along the ligament but rather different at different location and usually, the highest stresses are measured near the middle of the ligament [24, 25].

In all of the cases, the maximum principal stress steadily increased with the higher degrees of flexion in the knee and reached its maximum value at the end of the simulation, which was expected to happen since, the only possible source of strain is the rotation of the femur that is occurring, without any loads to simulate the weight of human body that the knee should be supporting or any other movement in any other plane of motion.

After successfully improving the features of the original model obtained from the Open Knee Project and obtaining this sufficiently stable and accurate model, it was used to get a sense of the kinematics of the knee joint, with all of its main anatomical structures, before the implementation of the UMAT with the damage parameter.

7.2 - Implementation of the HGO Material Model Using a UMAT with a Damage Parameter

After understanding the kinematics of the knee joint, the model was simplified and, as was previously mentioned, it was calibrated using the experimental environment of the paper of Paschos N.K. *et al.*, 2010 [104] which was recreated and the material and damage constants were adjusted until the obtained results were as close as possible to the graph obtained from the averaging of the experimental data. In order to test several parameters and reduce the computational cost of the simulation, a single cube was created (Figure 7.3), made up of a single

element, which was in turn made up of 8 nodes. The cube was stretched in order to replicate the experimental conditions and with it, it was possible to test the parameters in a uniform state of tension simulating a single element within the ACL.

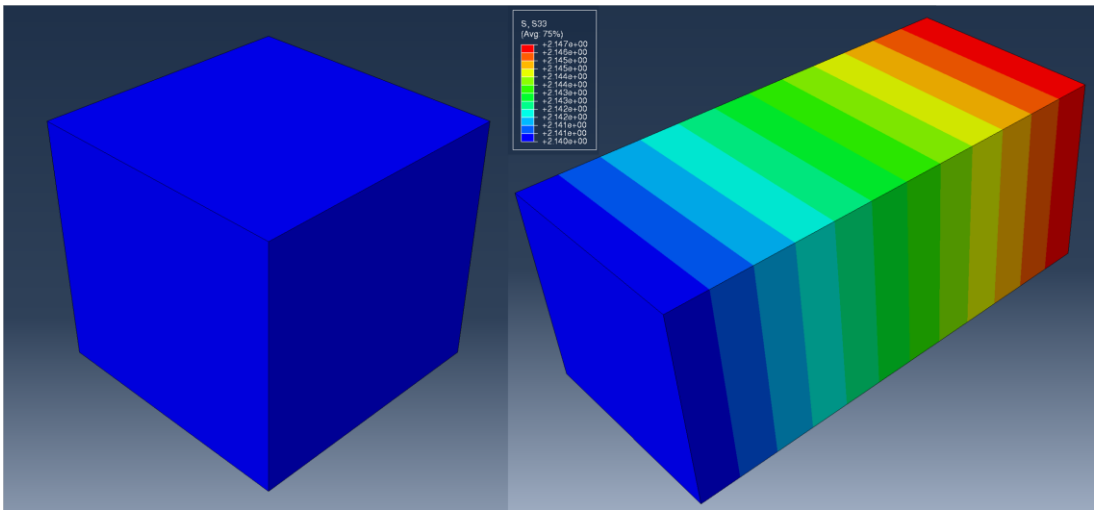

Figure 7.3 – Cube used in the calibration of the model.

After several tests, the parameters shown in Table 6.2, were chosen, since the stress curve which was obtained with them was as close as possible to the one obtained experimentally in the previously referenced paper, as shown in the figure below.

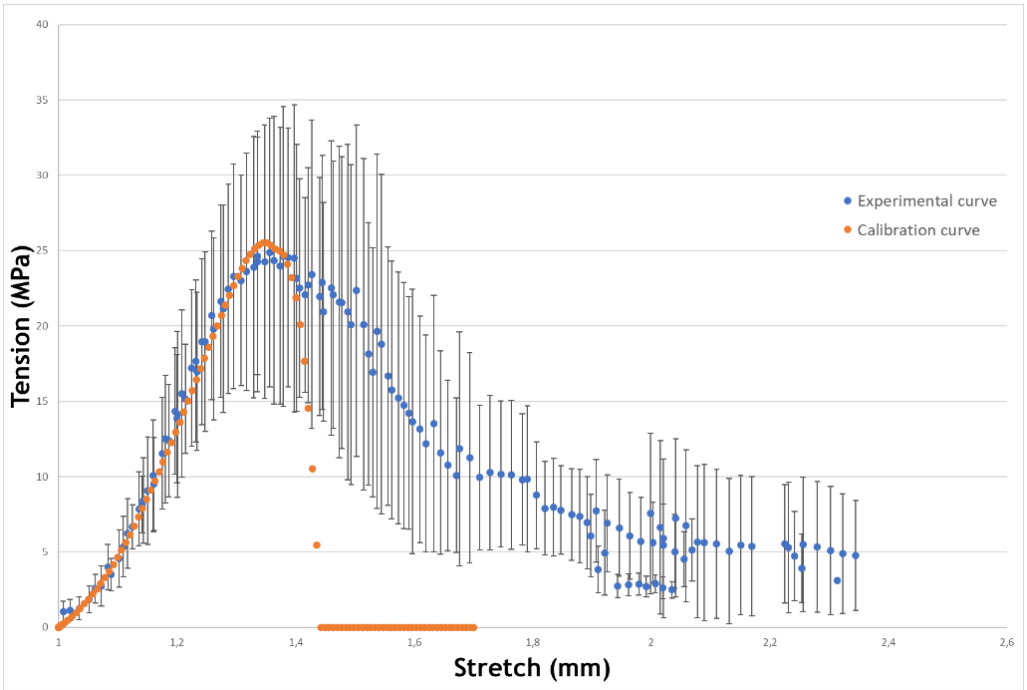

Figure 7.4 – Comparison between the figure created from the average of the experimental results presented in [104] (blue) and the results obtained from the calibration using the single element cube (orange).

7.3 - Evaluation of the Damage on the ACL in Injury Related Movements

The next stage in this work was to test some of the movements that are known to induce ACL injury, mentioned in Chapter 4.3. These were the anterior force at the tibia, knee valgus, a slight knee flexion and tibial internal rotation.

Based on the premise that the anterior force at the tibia is the main responsible for the ACL injury, this movement was tested alone and combined with all the other tested motions since, when combined with knee valgus, slight knee flexion or tibial internal rotation, it leads to more damage on the ligament.

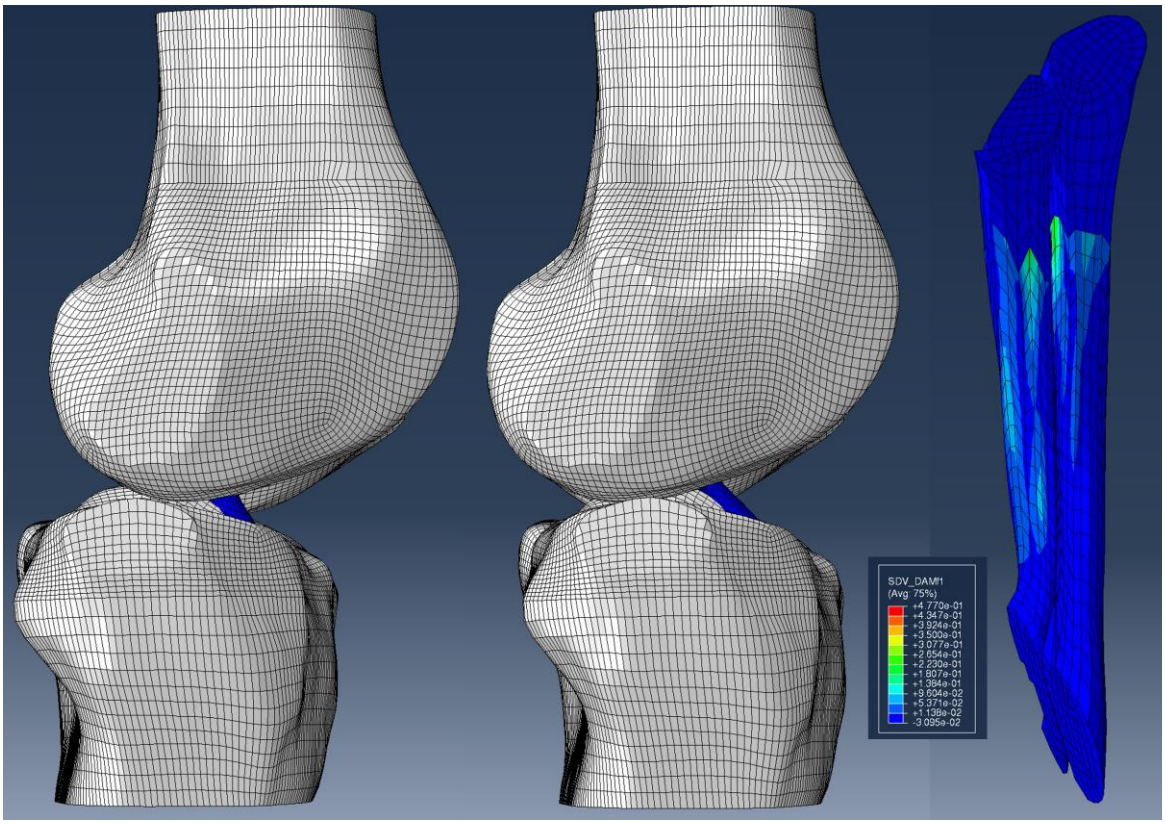

Figure 7.5 – Anterior translation of the tibia. Left – Neutral state; Middle – After anterior translation of the tibia; Right – Colour map of the representation the damage on the ACL (Lateral view).

In fact, this was also verified in the simulations, when isolated, the tibial anterior translation led to a damage which was, in some areas, around 47.88% and mostly located in the lateral side and posterior side of the ligament (Figure 7.5). When combined with either of the other movements (Figure 7.6), this percentage increased in every case. This increase was more pronounced in the case of the combination of the anterior translation with the knee valgus. This is in accordance with the existent bibliography which states that a combination of the anterior

translation of the tibia and one of these three other movements elicits higher strains on the ACL, especially in the case of the knee valgus [6, 70].

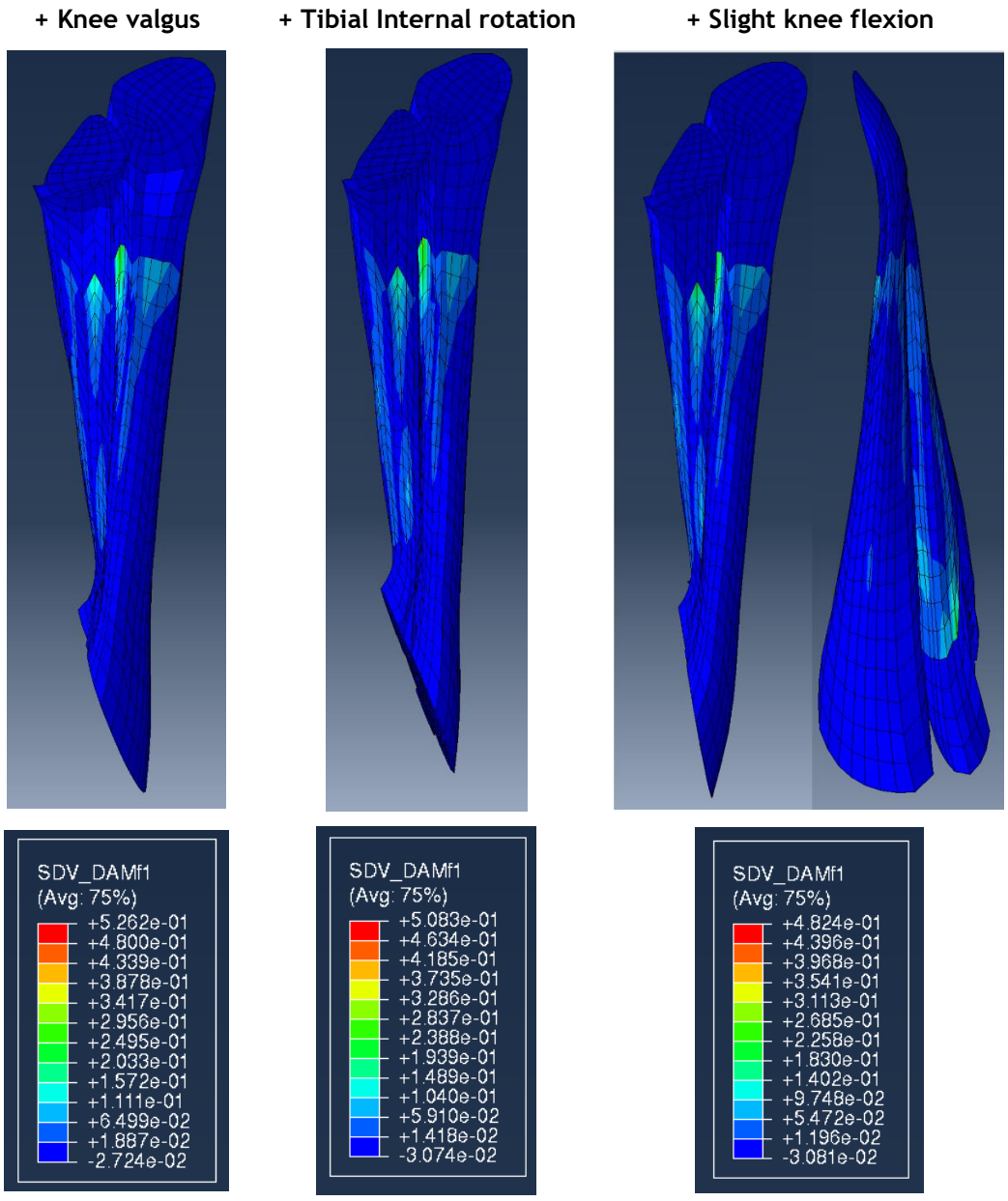

Figure 7.6 - Colour map of the representation the damage on the ACL (Lateral view) after the addition of knee valgus (left), tibial internal rotation (middle) and knee flexion (right) to the anterior translation movement.

Regarding the location of the damage, it is possible to notice that in the combination of the anterior translation and the knee valgus, the damage is mostly located at the lateral side of the ligament and prevalent in the AM bundle. In the PL bundle, there is a large area of damage that is present in its posterior side when the anterior translation is isolated (see Figure 7.5) which is absent in Figure 7.6. Regarding the addition of internal rotation, the location of the damage is

similar, the only real difference to the isolation of the anterior translation is the slight increase in the damage intensity. When analysing the addition of the slight knee flexion, it is possible to verify that the location of the damage was shifted to a more anterior location, especially in the PL bundle, which is noticeable in the additional picture which was added to Figure 7.6 in this case.

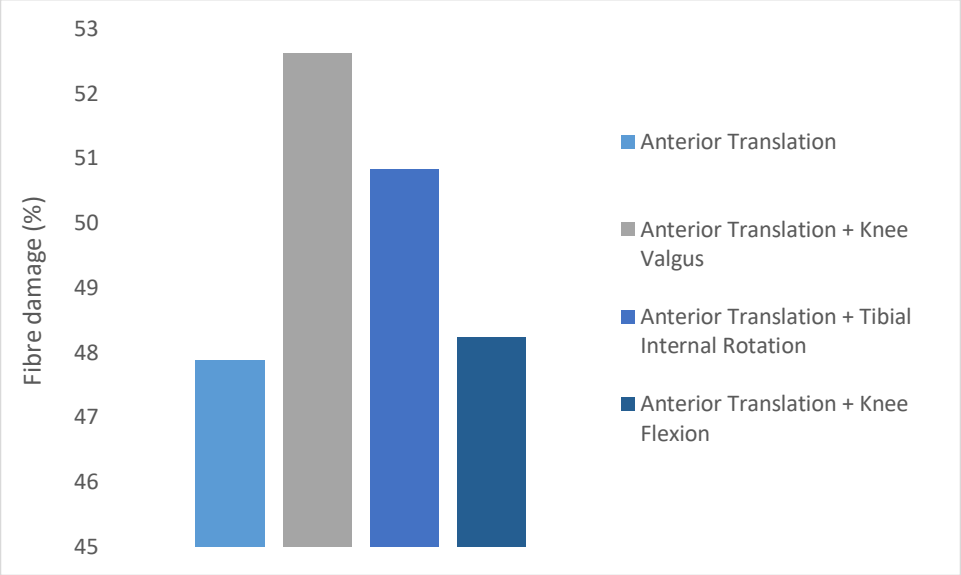

Figure 7.7 - Comparison between the highest achieved damage on the anterior translation and the highest achieved damage on the combination of this movement with the other secondary movements.

In Figure 7.7, it is possible to compare the influence of the different combinations. When the anterior translation is combined with one of the other three movements, the resulting damage always reaches higher values. It is also noteworthy that the combination with the knee valgus seems to elicit higher damages, while the combination with the knee flexion only leads to slight increase in the damage magnitude, indicating that simply combining it with the anterior translation does little difference in the overall damage to the ligament.

Several studies state that without the strain produced by the anterior translation of the tibia, the ACL injury cannot occur in a healthy knee. With this in mind, the valgus and flexion of the knee, as well as, the internal rotation of the tibia were evaluated individually, in order to confirm that the developed model was accurate and that their influence in the previous results is still noticeable when isolated.

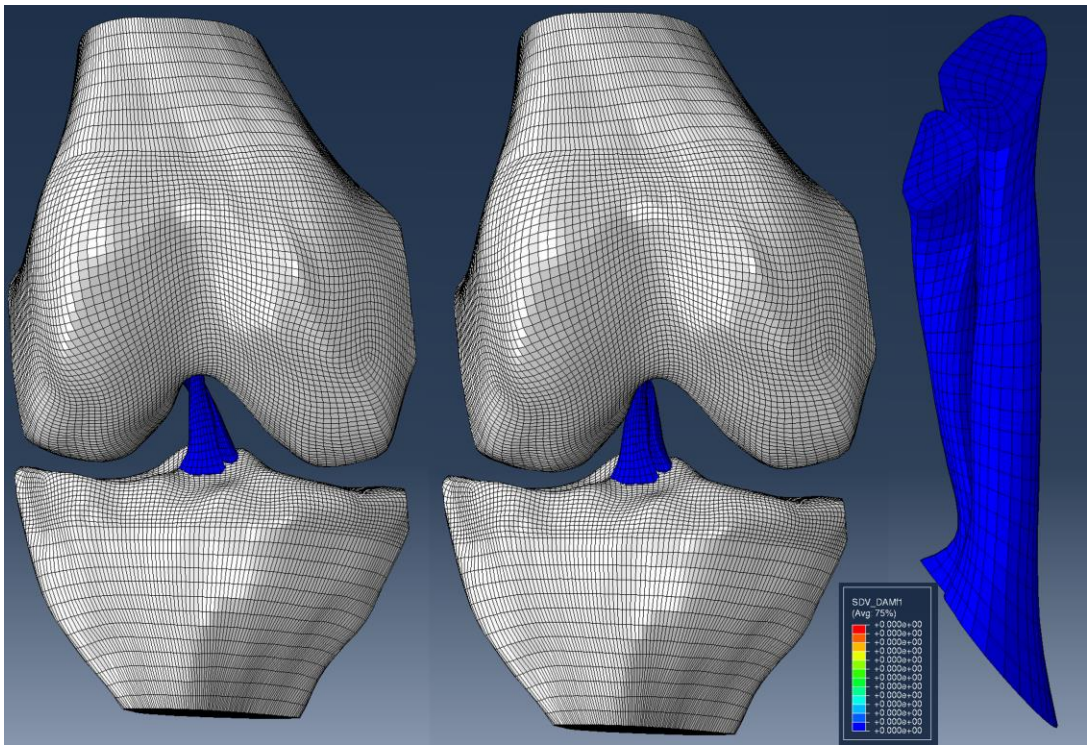

Figure 7.8 – Knee valgus. Left – Neutral state; Middle – After knee valgus; Right – Colour map of the representation the damage on the ACL (Lateral view).

In Figure 7.8 and Figure 7.10, it is noticeable that the isolation of both the knee valgus and the knee flexion did not lead to the occurrence of any damage on either bundle of the ACL, which is in accordance with the premise that, without the anterior translation movement the ACL injury does not occur.

Regarding the tibial internal rotation (Figure 7.9), there was some damage, probably resulting from the fact that the knee valgus and knee flexion are movements which are somewhat common in the normal functioning of the knee joint, while the tibial internal rotation is something more unlikely to happen in the daily activity and probably generates higher tensions on the ACL. Even so, the damages were quite low, only reaching between 10 to 11% in a specific location in the ligament while in other locations the damage was much lower. When analysing this damage, as was expected from the conclusions drawn from the previous simulations, the location of most of it is similar to the location on the simulation of anterior translation (Figure 7.5), which is to say that it is mostly located in the lateral side of the AM and PL bundles. In regard to its magnitude, it is much smaller than in the anterior translation, reaching only a maximum of 11.83%. As expected, the damage contribution from the anterior translation is much higher.

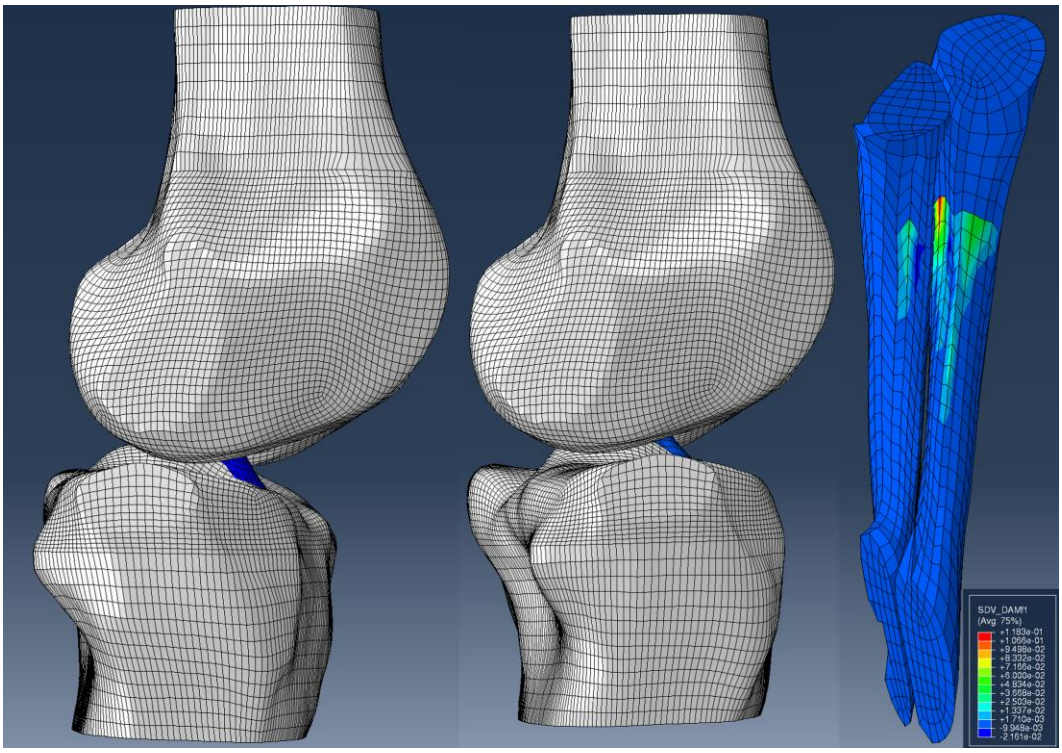

Figure 7.9 – Tibial internal rotation. Left – Neutral state; Middle – After tibial internal rotation; Right – Colour map of the representation the damage on the ACL (Lateral view).

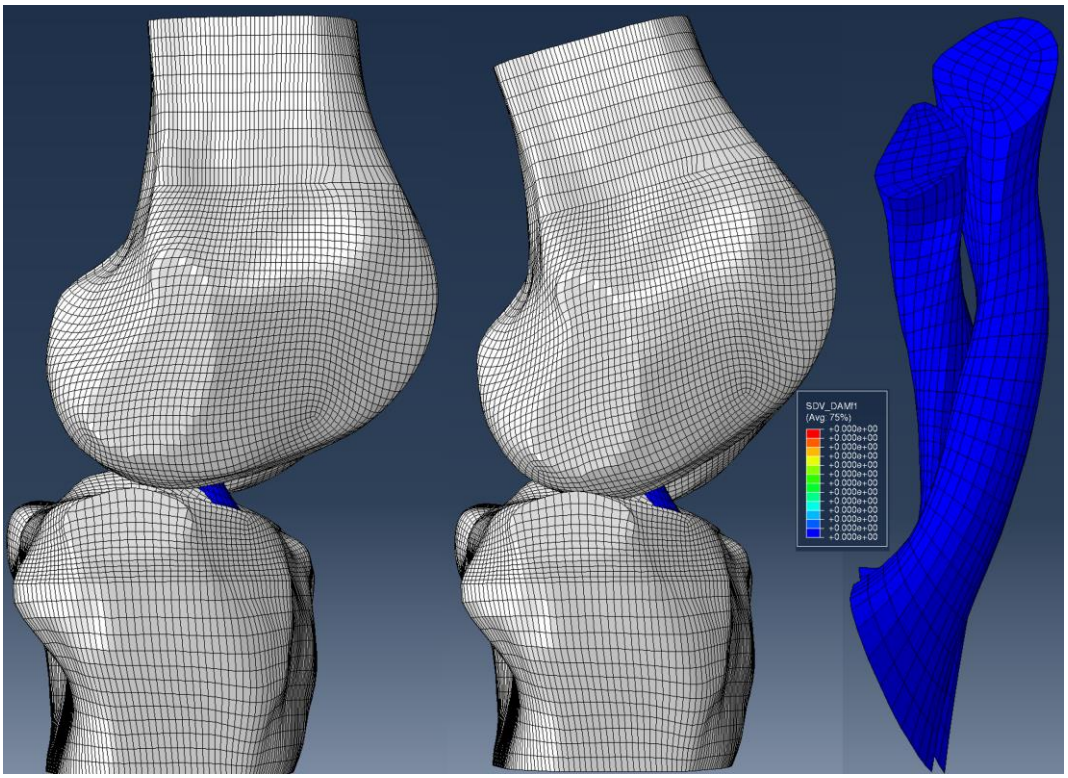

Figure 7.10 – Knee flexion. Left – Neutral state; Middle – After knee flexion; Right – Colour map of the representation the damage on the ACL (Lateral view).

The combination of movements involving the tibial anterior translation and knee flexion is quite common when an ACL injury occurs, therefore tow new simulations were performed where it was combined with both the knee valgus (the combination of these three motions is quite common in the landing portion of jumps that are associated with ACL injury) and with tibial internal rotation. The results of both simulations are shown in Figure 7.11. In the first case, it is possible to notice that the addition of the valgus movement led to a damage of higher magnitude (up to 55.43%) and the location of the damage was shifted, it became less prominent in the posterior area while being more concentrated on the lateral side of the ligament. Again, this shows the tendency for the knee valgus to concentrate the damage on the lateral side of the ligament.

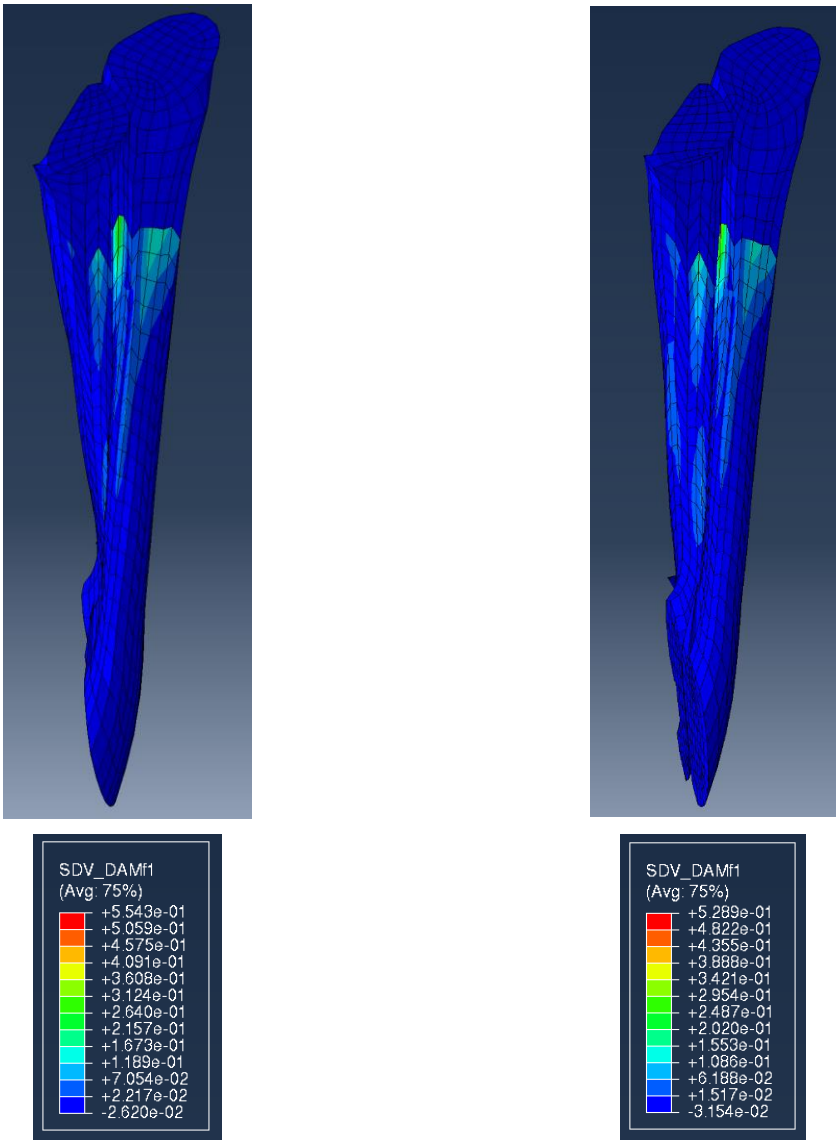

Figure 7.11 – Colour map of the representation the damage on the ACL (Lateral view). Left – Anterior translation combined with knee flexion and knee valgus; Right – Anterior translation combined with knee flexion and tibial internal rotation

With the addition of the tibial internal rotation, the damage was only amplified (reaching 53.89%) while the location remained similar. This is in agreement with previous simulations since the tibial translation and internal rotation both tend to damage the lateral portion of the ligament.

The last movement that was tested was the cutting movement. It can be described as a sudden change of direction to the side and is one of the most common movements that are performed during physical activity. It is also one of the most commonly performed movements in cases of ACL tear. It involves all of the motions which were previously tested, the knee is at a valgus motion, the quadricep is pulling the tibia anteriorly in order to slow down the momentum of the body, the knee is slightly flexed and there is internal tibial rotation, which can be quite significant in cases where the foot gets stuck on the ground during this movement.

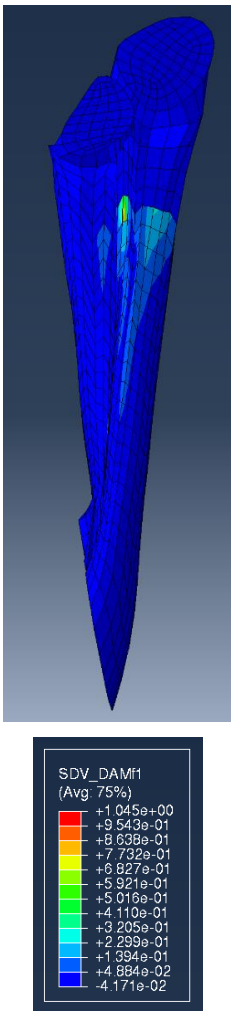

Figure 7.12 - Colour map of the representation the damage on the ACL (Lateral view) after performing the cutting movement.

In this case, the magnitude of the damage reached 104.5% in some points (Figure 7.12), which means that there was complete fibre rupture. The damage should be interpreted as 100% since the formula that is used to calculate the damage does not assume values higher than this, the

extra 4.5% is due to the extrapolation from the Gauss points into the nodes, done by the Abaqus software. This means that the combination of these four movements is more likely to cause ACL injury than in the absence of any of them. The location of the damage is once again focused on the lateral side of the ligament.

All of the results obtained from the several movements that were tested in this work are summarized in the table below.

Table 7.1 - Summary of the results obtained from the evaluation of the damage on the ACL in injury related movements.

Movements	Location of Most of the Damage	Highest Damage Value
Anterior Translation	Lateral and Posterior side	47.88%
Anterior Translation + Knee Valgus	Lateral side	52.62%
Anterior Translation + Tibial Internal Rotation	Lateral and Posterior side	50.83%
Anterior Translation + Knee Flexion	Lateral and Anterior side	48.24%
Knee Valgus	No damage	-
Tibial Internal Rotation	Lateral side	11.83%
Knee Flexion	No damage	-
Anterior Translation + Knee Flexion + Knee Valgus	Lateral side	55.43%
Anterior Translation + Knee Flexion + Tibial Internal Rotation	Lateral side	52.89%
Cutting Movement	Lateral	100%

Chapter 8 - Conclusion

The ACL injury is a condition that affects numerous people every year, especially athletes and people that lead an active lifestyle. It often demands long recovery periods and can, depending on the degree of the injury, require invasive reconstructive surgery. Due to its importance in the stabilization of the knee joint, an ACL injury can also lead to injuries in other structures and cause severe disabilities. Understanding the mechanism behind these injuries is an essential step in developing methods to prevent it.

In the literature there are several examples of the use of the FEM for the study of the ACL and of the injuries that afflict it, as well as the surgical procedures to repair it. So far, it has been established that the ACL injury occurs when an excessive tension is applied to it, which causes a tear. The ACL injury seems to result from a combination of forces and moments, of which, an anterior shear force on the proximal end of the tibia, caused by a strong contraction of the quadriceps muscle, seems to be the main factor. Knee valgus seems to have an important contribution to it, since most of the injuries happen when it is present. Another important factor is the knee at or near full extension at the time of injury, and tibial internal rotation. However, the exact mechanism behind this injury has yet to be fully understood.

In this work, a simplified model of the knee joint was subjected to several combinations of the movements which have been identified in several other studies as the main causes of ACL injury. The obtained results were in accordance with what is expected to happen in a real life ACL. The anterior translation of the tibia was clearly the main cause of damage and its combination with the other secondary movements further increased the damage on the ligament, especially with the valgus motion. In fact, the more secondary movements were added, the more the damage magnitude was increased, with the combination of all four movements being the one which generated damages of higher magnitude. This further proves the high complexity of the mechanism behind this injury.

Regarding the location of the damage, in general it is always located in the middle of the ligament which is in agreement with the fact that most of these injuries occur in the middle portion of the ACL, as was mentioned earlier. Within this middle portion, the damage was more prevalent in the lateral side of the ligament. When the anterior translation of the tibia is isolated, it leads

to the appearance of large damage areas in the lateral and posterior side of the ligament. This damage area on the posterior side seems to disappear with the addition of the valgus motion which focuses the damage on the lateral side. The addition of the tibial internal rotation to the anterior translation seems to focus the damage on the lateral side of the ACL. Finally, the addition of the knee flexion to the anterior translation leads to the appearance of a large damage area on the anterior side of the ligament, especially in the posterior bundle.

However, the obtained results are not without their limitations. Even though the kinematics imposed on the UMAT model were tested on a more complete model, the strains which the damage parameter used to apply the damage to the ligament, are likely not a completely accurate representation of the real strains that the ACL is subjected to, due to the absence of many of the main anatomical structures which are vital to the stabilization and structural integrity of this joint. Another limitation is the fact that a single family of fibres was included in the ligament, which means that all of the fibres had a similar orientation, which is not the case in a real ACL. In fact, some authors have gone as far as saying that the absence of the peripheral tissues of the knee joint, which is also the case in the models used in this work, may alter the joint biomechanics [105].

In conclusion, a stable and working finite element model was developed which included a UMAT capable of attributing the HGO material model to the ACL in conjugation with a damage parameter, which gives it the ability to simulate damage accumulation and predict the locations of fibre rupture in cases of injury. The model was adequately calibrated, which is confirmed by the satisfying results that were obtained when the model was subjected to kinematics which were obtained from a complete model of the knee joint with all of its main structures and with some improvements on the original Open knee model.

In future works, it would be interesting to enhance this geometric model with the inclusion of more anatomical structures of the knee and also attempt to test some of these movements related with the ACL injury with the inclusion of a vertical load which would simulate the weight of the individual. This would be particularly important in analysing movements such as the landing portion of a jump where an ACL tear is expected to occur, since many of these injuries stem from weight bearing motions such as this.

References

1. Standring, S., *Gray's anatomy e-book: the anatomical basis of clinical practice*. 2015, Elsevier Health Sciences. p. 1383-1397.
2. Ali, A.A., et al., *Combined measurement and modeling of specimen-specific knee mechanics for healthy and ACL-deficient conditions.* Journal of biomechanics, 2017. **57**: p. 117-124.
3. Kiapour, A., et al., *Finite element model of the knee for investigation of injury mechanisms: development and validation.* Journal of biomechanical engineering, 2014. **136**(1): p. 011002.
4. Woo, S.L.-Y., et al., *Biomechanics of knee ligaments: injury, healing, and repair.* Journal of biomechanics, 2006. **39**(1): p. 1-20.
5. McLean, S.G., K.F. Mallett, and E.M. Arruda, *Deconstructing the anterior cruciate ligament: what we know and do not know about function, material properties, and injury mechanics.* Journal of biomechanical engineering, 2015. **137**(2): p. 020906.
6. Aguilar, J. and J. Yang. *Anterior Cruciate Ligament (ACL) Injury: A Literature Review*. in *ASME 2017 International Design Engineering Technical Conferences and Computers and Information in Engineering Conference*. 2017. American Society of Mechanical Engineers Digital Collection.
7. Noyes, F.R. and S. Barber-Westin, *ACL injuries in the female athlete: causes, impacts, and conditioning programs*. 2018, Springer. p. 8-28.
8. Yu, B. and W.E. Garrett, *Mechanisms of non-contact ACL injuries.* British journal of sports medicine, 2007. **41**(suppl 1): p. i47-i51.
9. Boden, B.P., et al., *Non-contact ACL injuries: mechanisms and risk factors.* The Journal of the American Academy of Orthopaedic Surgeons, 2010. **18**(9): p. 520.
10. Wismans, J., et al., *A three-dimensional mathematical model of the knee-joint.* Journal of biomechanics, 1980. **13**(8): p. 677-685.
11. Cerniglia, D., et al., *FEM and experimental analysis of a total knee prosthesis.* 2018.
12. Kang, Y.-K., et al., *Analysis on Wear Phenomenon of Artificial Knee Joint Based on FEM and Mechanical Test.* International Journal of Precision Engineering and Manufacturing, 2018. **19**(8): p. 1211-1217.
13. Suyitno, P. and L. Pudjilaksono. *Experiment and FEM simulation of static test of knee joint prostheses*. in *American Institute of Physics Conference Series*. 2018.
14. Guo, H., et al., *A statistically-augmented computational platform for evaluating meniscal function.* Journal of biomechanics, 2015. **48**(8): p. 1444-1453.
15. Ren, D., et al., *The evaluation of the role of medial collateral ligament maintaining knee stability by a finite element analysis.* Journal of orthopaedic surgery and research, 2017. **12**(1): p. 64.

16. Xie, F., et al., *Effect of anterior cruciate ligament rupture of knee joint on meniscus and cartilage: a finite element analysis of knee joint.* Int J Clin Exp Med, 2017. **10**(12): p. 16468-16475.
17. Vairis, A., et al., *Evaluation of an intact, an ACL-deficient, and a reconstructed human knee joint finite element model.* Computer methods in biomechanics and biomedical engineering, 2016. **19**(3): p. 263-270.
18. Vairis, A., et al. *Studying the intact, ACL-deficient and reconstructed human knee joint using a finite element model*. in *ASME 2013 International Mechanical Engineering Congress and Exposition*. 2013. American Society of Mechanical Engineers Digital Collection.
19. Wang, H., et al., *Evaluation of a magnesium ring device for mechanical augmentation of a ruptured ACL: Finite element analysis.* Clinical Biomechanics, 2019.
20. Westermann, R.W., B.R. Wolf, and J.M. Elkins, *Effect of ACL reconstruction graft size on simulated Lachman testing: a finite element analysis.* The Iowa orthopaedic journal, 2013. **33**: p. 70.
21. Halonen, K., et al., *Optimal graft stiffness and pre-strain restore normal joint motion and cartilage responses in ACL reconstructed knee.* Journal of biomechanics, 2016. **49**(13): p. 2566-2576.
22. Park, H.-S., et al., *A knee-specific finite element analysis of the human anterior cruciate ligament impingement against the femoral intercondylar notch.* Journal of biomechanics, 2010. **43**(10): p. 2039-2042.
23. Orsi, A.D., et al., *The effects of knee joint kinematics on anterior cruciate ligament injury and articular cartilage damage.* Computer methods in biomechanics and biomedical engineering, 2016. **19**(5): p. 493-506.
24. Limbert, G., J. Middleton, and M. Taylor, *Finite element analysis of the human ACL subjected to passive anterior tibial loads.* Computer methods in biomechanics and biomedical engineering, 2004. **7**(1): p. 1-8.
25. Limbert, G., M. Taylor, and J. Middleton, *Three-dimensional finite element modelling of the human ACL: simulation of passive knee flexion with a stressed and stress-free ACL.* Journal of biomechanics, 2004. **37**(11): p. 1723-1731.
26. Xie, F., et al., *A study on construction three-dimensional nonlinear finite element model and stress distribution analysis of anterior cruciate ligament.* Journal of Biomechanical Engineering, 2009. **131**(12): p. 121007.
27. Song, Y., et al., *A three-dimensional finite element model of the human anterior cruciate ligament: a computational analysis with experimental validation.* Journal of biomechanics, 2004. **37**(3): p. 383-390.
28. Wan, C., Z. Hao, and S. Wen, *The effect of the variation in ACL constitutive model on joint kinematics and biomechanics under different loads: a finite element study.* Journal of biomechanical engineering, 2013. **135**(4): p. 041002.
29. Cooper, R.J., R.K. Wilcox, and A.C. Jones, *Finite element models of the tibiofemoral joint: A review of validation approaches and modelling challenges.* Medical engineering & physics, 2019.
30. Kazemi, M., Y. Dabiri, and L. Li, *Recent advances in computational mechanics of the human knee joint.* Computational and mathematical methods in medicine, 2013. **2013**.
31. Beidokhti, H.N., et al., *The influence of ligament modelling strategies on the predictive capability of finite element models of the human knee joint.* Journal of biomechanics, 2017. **65**: p. 1-11.
32. Mootanah, R., et al., *Development and validation of a computational model of the knee joint for the evaluation of surgical treatments for osteoarthritis.* Computer methods in biomechanics and biomedical engineering, 2014. **17**(13): p. 1502-1517.
33. Li, W., *Damage models for soft tissues: a survey.* Journal of medical and biological engineering, 2016. **36**(3): p. 285-307.

34. Waffenschmidt, T., et al., *A gradient-enhanced large-deformation continuum damage model for fibre-reinforced materials.* Computer Methods in Applied Mechanics and Engineering, 2014. **268**: p. 801-842.
35. Schmidt, T., D. Balzani, and G.A. Holzapfel, *Statistical approach for a continuum description of damage evolution in soft collagenous tissues.* Computer Methods in Applied Mechanics and Engineering, 2014. **278**: p. 41-61.
36. Volokh, K., *Modeling failure of soft anisotropic materials with application to arteries.* Journal of the Mechanical Behavior of Biomedical Materials, 2011. **4**(8): p. 1582-1594.
37. Forestiero, A., E. Carniel, and A. Natali, *Biomechanical behaviour of ankle ligaments: constitutive formulation and numerical modelling.* Computer methods in biomechanics and biomedical engineering, 2014. **17**(4): p. 395-404.
38. De Vita, R. and W.S. Slaughter, *A constitutive law for the failure behavior of medial collateral ligaments.* Biomechanics and modeling in mechanobiology, 2007. **6**(3): p. 189-197.
39. Guo, Z. and R. De Vita, *Probabilistic constitutive law for damage in ligaments.* Medical engineering & physics, 2009. **31**(9): p. 1104-1109.
40. Martini, F., et al., *Human anatomy*. 2003, Prentice Hall Upper Saddle River, NJ. p. 16-19.
41. VanPutte, C., *Seeley's anatomy & physiology*. 2016, McGraw-Hill Higher Education. p. 14-17; 254-257.
42. Tate, P., *Seeley's principles of anatomy and physiology*. 2011, McGraw-Hill Higher Education. p. 177-181.
43. Marieb, E.N. and K. Hoehn, *Human anatomy & physiology*. 2013, Pearson Education. p. 249-263.
44. Schuenke, M., E. Schulte, and U. Schumacher, *Atlas of anatomy*. 2016, Thieme. p. 428-435.
45. Chhabra, A., C.C. Elliott, and M.D. Miller, *Normal anatomy and biomechanics of the knee.* Sports medicine and arthroscopy review, 2001. **9**(3): p. 166-177.
46. Flandry, F. and G. Hommel, *Normal anatomy and biomechanics of the knee.* Sports medicine and arthroscopy review, 2011. **19**(2): p. 82-92.
47. Thompson, W.O., et al., *Tibial meniscal dynamics using three-dimensional reconstruction of magnetic resonance images.* The American journal of sports medicine, 1991. **19**(3): p. 210-216.
48. McDermott, I.D., S.D. Masouros, and A.A. Amis, *Biomechanics of the menisci of the knee.* Current Orthopaedics, 2008. **22**(3): p. 193-201.
49. Duthon, V., et al., *Anatomy of the anterior cruciate ligament.* Knee surgery, sports traumatology, arthroscopy, 2006. **14**(3): p. 204-213.
50. Goldblatt, J.P. and J.C. Richmond, *Anatomy and biomechanics of the knee.* Operative Techniques in Sports Medicine, 2003. **11**(3): p. 172-186.
51. Abulhasan, J.F. and M.J. Grey, *Anatomy and physiology of knee stability.* Journal of Functional Morphology and Kinesiology, 2017. **2**(4): p. 34.
52. Meyler, Z. *Knee Anatomy*. 2018 October 16, 2019]; Available from: https://www.arthritis-health.com/types/joint-anatomy/knee-anatomy.
53. Woo, S.L., et al., *Biomechanics of knee ligaments.* The American journal of sports medicine, 1999. **27**(4): p. 533-543.
54. Komdeur, P., F.E. Pollo, and R.W. Jackson. *Dynamic knee motion in anterior cruciate impairment: a report and case study*. in *Baylor University Medical Center Proceedings*. 2002. Taylor & Francis.
55. Jakob, R.P. and H. Stäubli, *The Knee and the cruciate ligaments: anatomy, biomechanics, clinical aspects, reconstruction, complications, rehabilitation*. 1992, Springer. p. 30-47.
56. Andriacchi, T.P., T.S. Stanwyck, and J.O. Galante, *Knee biomechanics and total knee replacement.* The Journal of arthroplasty, 1986. **1**(3): p. 211-219.

57. Dargel, J., et al., *Biomechanics of the anterior cruciate ligament and implications for surgical reconstruction.* Strategies in Trauma and Limb Reconstruction, 2007. **2**(1): p. 1-12.
58. Freeman, M.A. and V. Pinskerova, *The movement of the normal tibio-femoral joint.* Journal of biomechanics, 2005. **38**(2): p. 197-208.
59. Beasley, L.S., et al., *Anterior cruciate ligament reconstruction: A literature review of the anatomy, biomechanics, surgical considerations, and clinical outcomes.* Operative techniques in orthopaedics, 2005. **15**(1): p. 5-19.
60. Skelley, N.W., S.P. Lake, and R.H. Brophy, *Microstructural properties of the anterior cruciate ligament.* Annals of Joint, 2017. **2**(5).
61. Bicer, E.K., R.A. Magnussen, and P. Neyret, *Intra-articular landmarks for anterior cruciate ligament reconstructions: a review.* International Journal of Clinical Rheumatology, 2010. **5**(6): p. 677.
62. Markatos, K., et al., *The anatomy of the ACL and its importance in ACL reconstruction.* European Journal of Orthopaedic Surgery & Traumatology, 2013. **23**(7): p. 747-752.
63. Marieswaran, M., et al., *A review on biomechanics of anterior cruciate ligament and materials for reconstruction.* Applied bionics and biomechanics, 2018. **2018**.
64. Siegel, L., C. Vandenakker-Albanese, and D. Siegel, *Anterior cruciate ligament injuries: anatomy, physiology, biomechanics, and management.* Clinical Journal of Sport Medicine, 2012. **22**(4): p. 349-355.
65. Hall, S., *Basic biomechanics*. 2014, McGraw-Hill Higher Education. p. 239-242.
66. Wetters, N., et al., *Mechanism of injury and risk factors for anterior cruciate ligament injury.* Operative Techniques in Sports Medicine, 2016. **24**(1): p. 2-6.
67. Thambyah, A. *A biomechanical interpretation of the non-contact anterior cruciate ligament injury*. in *2012 IEEE-EMBS Conference on Biomedical Engineering and Sciences*. 2012. IEEE.
68. Dai, B., et al., *Anterior cruciate ligament injuries in soccer: Loading mechanisms, risk factors, and prevention programs.* Journal of Sport and Health Science, 2014. **3**(4): p. 299-306.
69. DeMorat, G., et al., *Aggressive quadriceps loading can induce noncontact anterior cruciate ligament injury.* The American journal of sports medicine, 2004. **32**(2): p. 477-483.
70. Chaudhari, A.M. and T.P. Andriacchi, *The mechanical consequences of dynamic frontal plane limb alignment for non-contact ACL injury.* Journal of biomechanics, 2006. **39**(2): p. 330-338.
71. Lai, W.M., et al., *Introduction to continuum mechanics*. 2010, Butterworth-Heinemann.
72. Rudnicki, J.W., *Fundamentals of continuum mechanics*. 2014: John Wiley & Sons.
73. Mase, G.T., R.E. Smelser, and J.S. Rossmann, *Continuum mechanics for engineers*. 2020: CRC press.
74. Bower, A.F., *Applied mechanics of solids*. 2009: CRC press.
75. Adeeb, S., *Introduction to solid mechanics and finite element analysis using Mathematica*. 2011: Kendall Hunt.
76. Gonzalez, O. and A.M. Stuart, *A first course in continuum mechanics*. 2008: Cambridge University Press.
77. Bonet, J. and R.D. Wood, *Nonlinear continuum mechanics for finite element analysis*. 2008: Cambridge university press.
78. Holzapfel, A.G., *Nonlinear solid mechanics: A Continuum Approach for Engineering*. 2001.
79. Dourte, L.M., A.F. Kuntz, and L.J. Soslowsky, *Twenty-five years of tendon and ligament research.* Journal of Orthopaedic Research, 2008. **26**(10): p. 1297-1305.
80. Mokhtari, M., et al., *Transversely isotropic viscoelastic materials: Contact mechanics and friction.* Tribology international, 2016. **97**: p. 116-123.
81. Belinha, J., *Meshless methods in biomechanics*, in *Bone Tissue Remodelling Analysis*. 2014. p. 15-39.

82. Liu, G.-R. and S.S. Quek, *The finite element method: a practical course*. 2013, Butterworth-Heinemann.
83. Peyroteo, M., et al., *Mechanical bone remodelling: Comparative study of distinct numerical approaches.* Engineering Analysis with Boundary Elements, 2019. **100**: p. 125-139.
84. Turner, M., *Stiffness and deflection analysis of complex structures.* journal of the Aeronautical Sciences, 1956. **23**(9): p. 805-823.
85. Eslami, M.R., *Finite elements methods in mechanics*. 2014: Springer.
86. Jacob, F. and B. Ted, *A first course in finite elements*. 2007: Wiley.
87. Zienkiewicz, O.C., R.L. Taylor, and J.Z. Zhu, *The finite element method: its basis and fundamentals*. 2005: Elsevier.
88. Haut Donahue, T.L., et al., *A finite element model of the human knee joint for the study of tibio-femoral contact.* J. Biomech. Eng., 2002. **124**(3): p. 273-280.
89. Erdemir, A. and S. Sibole, *Open knee: a three-dimensional finite element representation of the knee joint.* User's guide, version, 2010. **1**(0).
90. Erdemir, A., *Open knee: open source modeling and simulation in knee biomechanics.* The journal of knee surgery, 2016. **29**(02): p. 107-116.
91. Shriram, D., et al., *Evaluating the effects of material properties of artificial meniscal implant in the human knee joint using finite element analysis.* Scientific reports, 2017. **7**(1): p. 6011.
92. Łuczkiewicz, P., et al., *The influence of articular cartilage thickness reduction on meniscus biomechanics.* PloS one, 2016. **11**(12): p. e0167733.
93. Khoshgoftar, M., et al., *The sensitivity of cartilage contact pressures in the knee joint to the size and shape of an anatomically shaped meniscal implant.* Journal of biomechanics, 2015. **48**(8): p. 1427-1435.
94. Completo, A., et al., *Biomechanical Evidence on Anterior Cruciate Ligament Reconstruction.* Revista Brasileira de Ortopedia, 2019. **54**(2): p. 190-197.
95. Freutel, M., et al., *Finite element modeling of soft tissues: material models, tissue interaction and challenges.* Clinical Biomechanics, 2014. **29**(4): p. 363-372.
96. Pena, E., et al., *A three-dimensional finite element analysis of the combined behavior of ligaments and menisci in the healthy human knee joint.* Journal of biomechanics, 2006. **39**(9): p. 1686-1701.
97. Li, G., O. Lopez, and H. Rubash, *Variability of a three-dimensional finite element model constructed using magnetic resonance images of a knee for joint contact stress analysis.* J. Biomech. Eng., 2001. **123**(4): p. 341-346.
98. Spilker, R.L., P.S. Donzelli, and V.C. Mow, *A transversely isotropic biphasic finite element model of the meniscus.* Journal of biomechanics, 1992. **25**(9): p. 1027-1045.
99. LeRoux, M.A. and L.A. Setton, *Experimental and biphasic FEM determinations of the material properties and hydraulic permeability of the meniscus in tension.* J. Biomech. Eng., 2002. **124**(3): p. 315-321.
100. Skacel, P. and J. Bursa, *Comparison of constitutive models of arterial layers with distributed collagen fibre orientations.* Acta of bioengineering and biomechanics, 2014. **16**(3).
101. Holzapfel, G.A., T.C. Gasser, and R.W. Ogden, *Comparison of a multi-layer structural model for arterial walls with a Fung-type model, and issues of material stability.* Journal of biomechanical engineering, 2004. **126**(2): p. 264-275.
102. Ferreira, J., et al., *A general framework for the numerical implementation of anisotropic hyperelastic material models including non-local damage.* Biomechanics and modeling in mechanobiology, 2017. **16**(4): p. 1119-1140.
103. Calvo, B., et al., *An uncoupled directional damage model for fibred biological soft tissues. Formulation and computational aspects.* International journal for numerical methods in engineering, 2007. **69**(10): p. 2036-2057.

104. Paschos, N.K., et al., *Cadaveric study of anterior cruciate ligament failure patterns under uniaxial tension along the ligament.* Arthroscopy: The Journal of Arthroscopic & Related Surgery, 2010. **26**(7): p. 957-967.
105. Beidokhti, H.N., et al., *The peripheral soft tissues should not be ignored in the finite element models of the human knee joint.* Medical & biological engineering & computing, 2018. **56**(7): p. 1189-1199.

Appendix

```
%%%%%%%%%%%%%%%%%%%%%%%%%%%%%%%%%%%%%%%%%%%%%%%%%%%%%%%%%%%%%%%%%%%%%%%%%%%%%%%%
clc;
clf;
clear;
load nodes.dat
load elements.dat
%load familia_fibras1.dat
%load familia_fibras2.dat
tabela=zeros(3000,4);
id=elements(:,1);
tabela(:,1)=id;
node_inicial=elements(:,2);
node_final=elements(:,6);
idnode=nodes(:,1);
tabelaxyz_node_inicial=zeros(3000,4);
tabelaxyz_node_final=zeros(3000,4);
j=0;
tabelaxyz_node_inicial(:,1)=node_inicial;
tabelaxyz_node_final(:,1)=node_final;
norma=zeros(3000,1);
nelem=3000;
centroids=zeros(nelem,3);

angle1=29;
angle2=62;

vetoresfinais=zeros(3000,3);


%para no 1
for i=1:3000
```

```
    for j=1:5084
        if node_inicial(i,1) == nodes(j,1)

          tabelaxyz_node_inicial (i,2) = nodes(j,2);
          tabelaxyz_node_inicial (i,3) = nodes(j,3);
          tabelaxyz_node_inicial (i,4) = nodes(j,4);


    end
    end
end

%para no 4
for i=1:3000
    for j=1:5084
        if node_final(i,1) == nodes(j,1)

          tabelaxyz_node_final (i,2) = nodes(j,2);
          tabelaxyz_node_final (i,3) = nodes(j,3);
          tabelaxyz_node_final (i,4) = nodes(j,4);


    end
    end
end

%norma e xyz

for k=1:3000
    norma(k,1)=sqrt(((tabelaxyz_node_inicial(k,2)-tabelaxyz_node_final(k,2))^2)+((tabelaxyz_node_inicial(k,3)-
tabelaxyz_node_final(k,3))^2)+((tabelaxyz_node_inicial(k,4)-tabelaxyz_node_final(k,4))^2));
    tabela(k,2)=(tabelaxyz_node_inicial(k,2)-tabelaxyz_node_final(k,2))/(norma(k,1));
    tabela(k,3)=(tabelaxyz_node_inicial(k,3)-tabelaxyz_node_final(k,3))/(norma(k,1));
    tabela(k,4)=(tabelaxyz_node_inicial(k,4)-tabelaxyz_node_final(k,4))/(norma(k,1));
end

face1 = [1 2 3 4]; % vertices to connect to make square
face2 = [5 6 7 8];
face3 = [2 3 7 6];
face4 = [1 4 8 5];
face5 = [1 2 6 5];
face6 = [4 3 7 8];

nodes_coordinates=nodes(:,2:4);
elements_connectivities=elements(:,2:9);

for i=1:3000;
node_inicial=elements_connectivities(i,1);
node2=elements_connectivities(i,2);
node3=elements_connectivities(i,3);
```

```
node_final=elements_connectivities(i,4);
node_inicial=elements_connectivities(i,5);
node6=elements_connectivities(i,6);
node_final=elements_connectivities(i,7);
node8=elements_connectivities(i,8);

for ii=1:8
    nodei=elements_connectivities(i,ii);
    for jj=1:5084
        if nodei == nodes(jj,1);
            node(ii,:)=nodes(jj,2:4);
        end
    end
end
   centroid_x=(node(1,1)+node(2,1)+node(3,1)+node(4,1)+node(5,1)+node(6,1)+node(7,1)+node(8,1))/8;
   centroid_y=(node(1,2)+node(2,2)+node(3,2)+node(4,2)+node(5,2)+node(6,2)+node(7,2)+node(8,2))/8;
   centroid_z=(node(1,3)+node(2,3)+node(3,3)+node(4,3)+node(5,3)+node(6,3)+node(7,3)+node(8,3))/8;
   centroids(i,1)=centroid_x;
   centroids(i,2)=centroid_y;
   centroids(i,3)=centroid_z;


%node=[nodes_coordinates(node1,:) ;...
 %     nodes_coordinates(node2,:) ;...
  %    nodes_coordinates(node3,:) ;...
   %   nodes_coordinates(node4,:) ;...
    %  nodes_coordinates(node5,:) ;...
     %  nodes_coordinates(node6,:) ;...
       %nodes_coordinates(node7,:) ;...
       %nodes_coordinates(node8,:) ];




patch('Faces',face1,'Vertices',node,'FaceColor','none')
patch('Faces',face2,'Vertices',node,'FaceColor','none')
patch('Faces',face3,'Vertices',node,'FaceColor','none')
patch('Faces',face4,'Vertices',node,'FaceColor','none')
patch('Faces',face5,'Vertices',node,'FaceColor','none')
patch('Faces',face6,'Vertices',node,'FaceColor','none')

plot3(centroids(i,1),centroids(i,2),centroids(i,3),'o')



vetoresfinais(i,1)=tabela(i,2)+centroids(i,1);
vetoresfinais(i,2)=tabela(i,3)+centroids(i,2);
vetoresfinais(i,3)=tabela(i,4)+centroids(i,3);

quiver3(centroids(i,1),centroids(i,2),centroids(i,3),tabela(i,2),tabela(i,3),tabela(i,4),5.0);
```

```
axis equal;
axis square;
%axis([0 1.5 0 1.5 0 1.5])

hold on;

view(3);

title(['Cartesian Mesh'])
end
```